

Retrofitting offshore wind foundations with airborne wind energy systems

A techno-economic analysis

MSc thesis

Boris Messer

MSc Offshore and dredging engineering



©Boris Messer

Cover photo: Makani M600 AWE system mounted on a spar buoy and conventional wind turbine mounted on a monopile in Norway, autumn 2019. Image credits: Makani Power

Retrofitting offshore wind foundations with airborne wind energy systems

A techno-economic analysis

MSc thesis

Boris Messer
4565452

October 16, 2023

Thesis committee:

Ir. A.C.M. van der Stap,	TU Delft, chair
Dr. R. Schmehl,	TU Delft, daily supervisor
Ir. M. Mroczek,	DEME, daily supervisor

Abstract

This thesis explores the feasibility of retrofitting ageing offshore wind farm (OWF) foundations with airborne wind energy (AWE) systems as a sustainable alternative to decommissioning or wind turbine (WT) refurbishment. These OWFs, starting their operational life between 1995 and 2003, face the challenge of reaching the end of their 20 to 25-year lifespan. Decommissioning incurs costs and environmental concerns, while refurbishment with larger WTs is increasingly expensive due to rapid technological advancements.

The study conducts a structural assessment of retrofitting offshore foundations with a 500 kW AWE system, covering the ultimate limit state (ULS) and fatigue limit state (FLS) evaluations. ULS calculations confirm that the foundations can withstand new AWE-generated wind and wave loads without exceeding design limits. Fatigue assessments demonstrate substantial expected foundation lifespans, even with a 99% initial damage assumption, suggesting AWE retrofitting preserves structural integrity.

Other AWE retrofitting scenarios are considered as well. Retaining the tower and mounting the 500 kW AWE system atop the tower is deemed possible, resulting in higher capacity factors. Calculations using a 2MW AWE system are performed as well. This is structurally possible, but the AWE technology of that size still faces technological challenges.

The economic feasibility of AWE system retrofitting is assessed through income and cost evaluations, comparing it to repowering with larger WTs. Results indicate competitive LCoE values for tower-mounted AWE compared to WT repowering, offsetting decommissioning costs and promising sustainable energy generation. Notably, 2 MW AWE systems exhibit economic potential in various scenarios.

This research contributes valuable insights into the viability of AWE retrofitting for ageing OWFs with AWE technology, offering a sustainable pathway forward and highlighting both the possibilities and challenges of this approach.

Acknowledgements

I am deeply grateful to all the individuals who supported and guided me throughout this research project. Their contributions have been invaluable and instrumental in shaping the outcomes of this endeavour.

I want to express my sincere gratitude to my academic supervisors, Roland Schmehl and André van der Stap, for their guidance, expertise, and mentorship. Their academic insights into the airborne wind technology and offshore foundations, respectively, and constructive feedback played a crucial role in refining the direction of this research.

I am equally thankful to my company supervisors, Maciej Mroczek, Johan de Haan, and Majvil Bajrami, from DEME, for their remarkable support. Their practical insights, industry knowledge, and provision of resources greatly enriched the scope of this project.

Lastly, I extend my deepest gratitude to my family and friends for their unwavering support and understanding during this journey.

This project would not have been possible without the collaborative efforts of all those mentioned above. Thank you for believing in me and being a vital part of this significant accomplishment.

Delft University of Technology, 16-10-2023
Boris Messer

Abbreviations

AWE airborne wind energy.

BoP balance of plant.

DFE design fatigue factor.

EFL equivalent fatigue loads.

EoL end of life.

FE finite element.

FLS fatigue limit state.

LCoE levelized cost of energy.

MSL mean sea level.

MW megawatt.

NPV net present value.

OWF offshore wind farms.

RNA rotor nacelle assembly.

ULS ultimate limit state.

WT wind turbine.

Contents

Acknowledgements	5
Abbreviations	6
1 Introduction	9
2 Literature review	11
2.1 Airborne wind energy	11
2.1.1 Ground generating	11
2.1.2 Onboard generating	12
2.1.3 Fixed wing or soft wing	12
2.1.4 Airborne wind energy system selection	12
2.2 Retrofitting offshore wind farms	13
2.3 Foundation analysis	15
2.3.1 Fatigue of foundations	15
2.3.2 Loads and forces acting on the foundation	16
2.3.3 Tether forces due to wind loads	16
2.3.4 Wave loads	19
2.4 Economics	20
2.4.1 Economics of AWE	20
2.4.2 Cost of retrofitting	21
2.4.3 Maintenance	21
2.4.4 Market factors	22
2.4.5 Levelized cost of energy	22
2.4.6 NPV	23
2.5 Research question	23
3 Structural Reserves in Foundations	24
3.1 Loads	24
3.1.1 Tether loads	24
3.1.2 Wave loads	28
3.1.3 Wave load results	31
3.2 ULS	32
3.3 Fatigue of foundation	36
3.4 Expected lifetime	38
4 Optimization	40
4.1 Replacing RNA with AWE system	40
4.2 Larger AWE system	41
4.3 Larger AWE system replaces RNA	42
5 Economics	43
5.1 Income	43
5.2 Costs	47
5.2.1 AWE on foundation	47
5.2.2 AWE on tower	49
5.2.3 AWE maintenance	49
5.2.4 Repowering with 10MW WT	50

5.2.5	Only decommissioning	51
5.3	Results	51
5.3.1	Nysted	51
5.3.2	Horns Rev I	53
6	Economic optimization	54
6.1	Economics 2MW airborne wind energy system	54
6.2	Economics replacement 500kW AWE with 2MW AWE	55
6.3	Reduced discount rate	56
6.4	Results	56
7	Discussion	58
7.1	Limitations	58
7.1.1	Airbone wind energy system	58
7.1.2	Structural reserves	58
7.1.3	Economics	58
7.1.4	Modifications	59
7.2	Recommendations	59
7.2.1	Airborne wind energy	59
7.2.2	Structural reserves	60
7.2.3	Optimization	60
7.2.4	Economics	60
8	Conclusion	61
	References	63
A	S-N curves	67
B	Formula sheets	68
C	OWF locations	74
D	Structural limitations	76
D.1	Fatigue damage percentage	76
D.2	Tower reinforcements	76
E	Economic limitations	78
E.1	Discount rate	78
E.2	Development	79
E.3	Subsidy	79

1 Introduction

Since the beginning of the 21st century, there has been a significant increase in the deployment of offshore wind farms (OWF) [1]. The average lifespan of an OWF is between 20 and 25 years. In Europe, several OWFs were commissioned between 1995 and 2003 [2]. These are now 20 or more years in operation and, therefore, essentially at their end of life (EoL). A complete list is given in Table 1 below. A map with their respective locations can be found in Figure 37 in Appendix C.

OWF	Year of commissioning	Capacity (MW)	Number of turbines	WT power (MW)
1. Tuno Knob	1995	5	10	0.50
2. Bockstigen	1998	2.75	5	0.55
3. Blyth Offshore	2000	4	2	2
4. Middelgrunden	2000	40	20	2
5. Horns Rev I	2002	160	80	2
6. Nysted	2003	166	72	2.3
7. Samsø	2003	23	10	2.3
8. Ronland I	2003	17.2	8	2 - 2.3
9. Frederikshavn	2003	7.6	3	2.3 - 3
10. North Hoyle	2003	60	30	2

Table 1: OWFs with more than 20 years of operation [3]

Upon reaching the EoL, the decision must be made whether to decommission, refurbish or retrofit the OWF. The decommissioning of an entire wind farm involves considerable cost, not only in terms of finance but also in relation to the marine life that may have established habitats on the wind farm foundations [4]. Additionally, it is essential to consider that the support structure and foundation of a wind turbine (WT) significantly contribute to the levelized cost of energy [5]. While refurbishing WTs may be a possible solution, technological advancements in WT technology have made it considerably expensive to refurbish the turbines. Life extension by refurbishment is, therefore, not an economical solution [6].

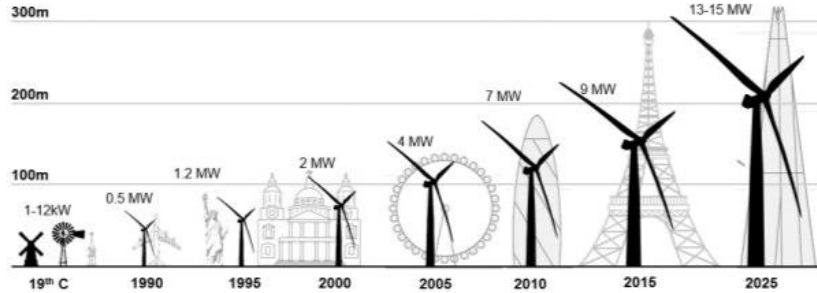


Figure 1: Evolution of WTs [7]

The technological advancements include an increase in size, which results in larger WTs. As turbine size has increased significantly over recent decades, older turbines are only a fraction of the size of modern ones [8], which is also clearly visible in Figure 1. In Table 1, it can be seen that the WTs in that period were around 2 megawatt (MW). In 2014, the average installed WT offshore was doubled to 4MW [9]. However, modern WTs are even larger. In 2022, the average installed offshore WT was 8MW and the average of newly ordered WTs is 12.2MW [9]. This dramatic increase in size over the last few years

also means that the foundations have increased in size. A monopile for a 2MW WT is typically 4.5m in diameter [10], while the diameter of the monopiles for 8MW WTs is typically around 8m [11]. This increase in pile diameter will only expand in the future to diameters of 10m or larger for the largest WTs [11]. Because of the increase in the size of the offshore WTs and, consequently, the increase in monopile size, retrofitting existing monopiles with modern WTs seems unlikely.

This raises the question of whether an alternative method of utilizing existing foundations is available, such as repowering them with airborne wind energy (AWE) systems. An AWE system provides energy with flying kites. The current sizes of various AWE systems are 100kW, and development towards a 500kW system is happening [12]. It could be interesting to retrofit the existing foundations with AWE systems because of different and potentially lower loads that will act on the foundations. The AWE systems can be easily set up and use less material than conventional wind energy [13]. Furthermore, this could be a cost-effective way to get AWE systems offshore and help to get funding for further development. Lastly, it would result in significant economic advantages since the foundations can stay in place. Retrofitting foundations with AWE systems also comes with challenges. A thorough inspection of the WT foundations is necessary to determine their ability to withstand loads, the AWE system must be able to work completely autonomously, and other modifications might also be needed [14]. In Figure 2, two examples are shown of how this would look. Figure 2a is a render by TwingTec and Figure 2b is an actual image by Makani.



(a) Rendering of TwingTec offshore [15]



(b) Makani M600 on offshore buoy [16]

Figure 2: Examples of AWE systems on offshore foundations

This study is divided into several sections. In Section 2, a review of the existing literature on the topic is provided, which includes a discussion of different AWE systems, the necessary methods for loads and fatigue, and the basics of economics. Based on this literature review, a research question and sub-questions are formulated to fill the discovered knowledge gap. Section 3 analyzes the structural reserve of the foundations to determine their viability for retrofitting OWFs with AWE systems. In Section 4, possible optimizations are validated structurally, building on the structural analysis from the previous chapter. Section 5 covers all the economics related to retrofitting with 500kW AWE compared to a competitive system. Section 6 analyses two additional economic optimizations involving 2MW AWE systems. In Section 7, recommendations for further research are provided. Finally, in Section 8, conclusions are drawn.

2 Literature review

2.1 Airborne wind energy

To comprehend the idea behind this research, it is crucial to have a fundamental understanding of the energy-generating component. This section provides a review of the concept behind the technology and a description of the AWE system used for this study.

AWE is a novel technology that captures wind energy from higher altitudes than conventional WTs. Generally, two principles are involved: ground generating and onboard generating. These are depicted in Figure 3[13]. These systems can be made with a fixed wing or a soft wing.

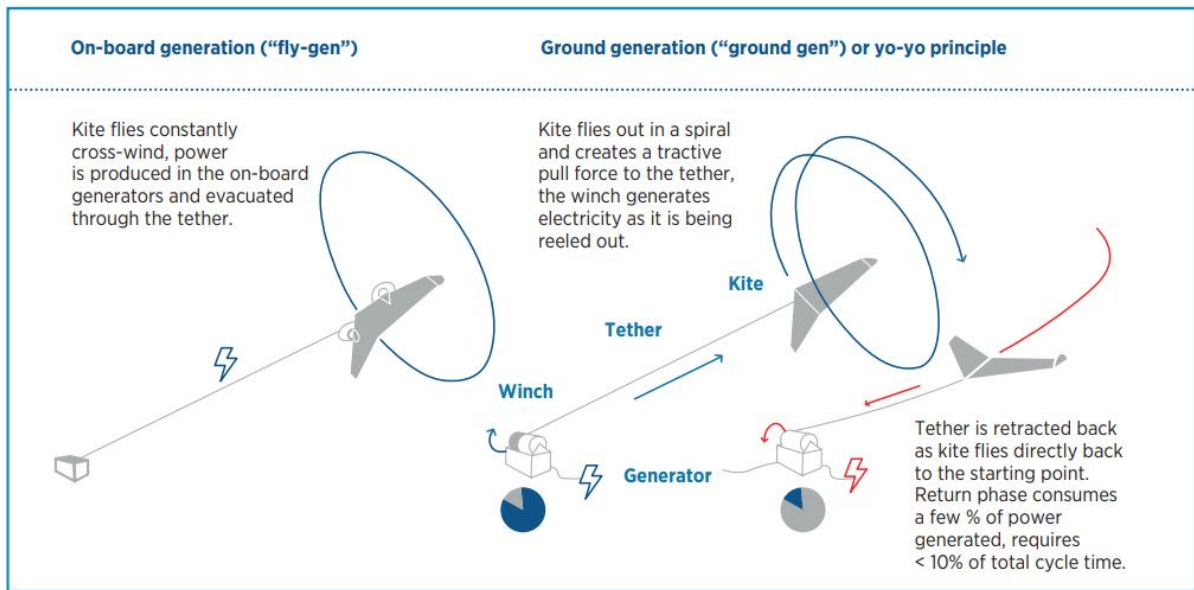


Figure 3: AWE operating principles [13]

2.1.1 Ground generating

The ground generating system is one of the most used and studied principles in airborne energy generation[17]. The potential of AWE is extensive because the kites can fly in a crosswind direction. In other words, it is perpendicular to the predominant wind direction. This results in higher velocities compared to conventional WTs [18]. The wind at higher altitudes is generally stronger. However, the air density decreases with altitude. This is not relevant for the altitudes of the AWE system used in this study. The kites generally fly at two or three times the altitude of conventional WTs, so the ratio between power and swept area is more optimised[18]. This is also visible in Figure 4. However, higher altitudes are not always better, as a longer tether and a larger elevation angle would be necessary, negatively impacting the energy production[19].

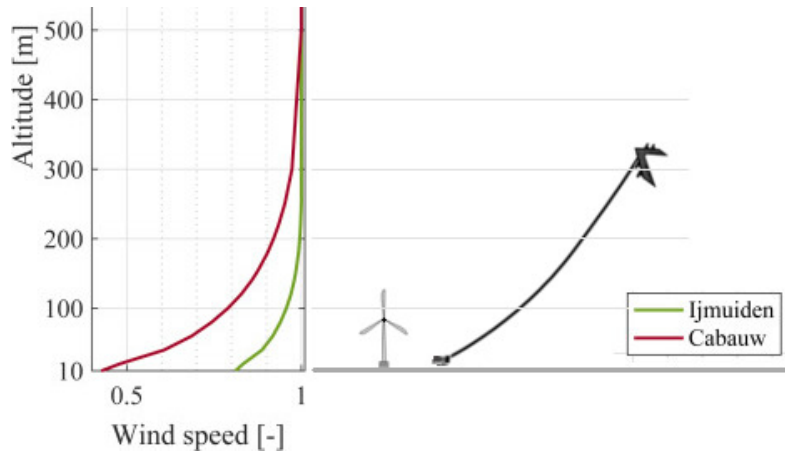


Figure 4: AWE vs WT and higher wind velocity at higher altitude, due to boundary layer[20]

2.1.2 Onboard generating

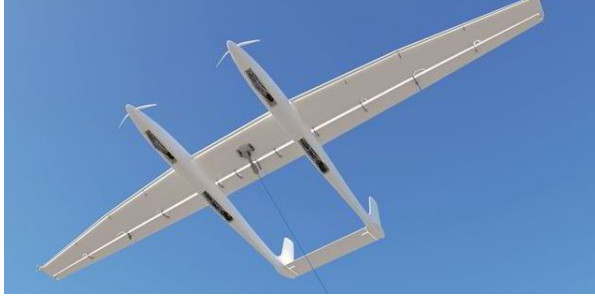
Another possibility for AWE to work is to generate electricity on board. The kite can still fly at high velocities in crosswind, similar to the ground-generating principle. However, in this case, the tether length is fixed to a certain length, and the turbines are onboard the kite. Due to the high apparent wind velocity at the kite, the onboard wind turbines can generate electricity[21]. This electricity is generated at the kite in the air. Therefore, the tether has to conduct the electricity to the ground station. In this case, higher altitudes are also not always better due to the increased tether length and larger elevation angle.

2.1.3 Fixed wing or soft wing

For the onboard generating principle, the kite has to be a fixed-wing kite due to the need for a structure that houses the electronics. The ground-generating principle, however, can use either a soft wing or a fixed wing. Both have their advantages and disadvantages. The benefits of a soft wing are their small weight, stable flight behaviour and low cost. The lightweight and stable flight behaviour makes the soft wing less hazardous[22, 23]. However, the disadvantages are their relatively poor depowering capabilities and their limited lifetime [22]. On the other side, there is the rigid-wing kite. The advantages of a fixed-wing kite are the aerodynamic benefit, ease of control, and higher durability. The largest disadvantage is the larger weight of the fixed-wing kite, which limits its performance with low winds [22].

2.1.4 Airborne wind energy system selection

In offshore conditions, the wind velocities are generally higher, and maintenance is complex due to the remote locations. The general absence of people around an OWF ensures safety, even when using a fixed-wing kite. Therefore, a fixed-wing kite is a logical choice for retrofitting offshore foundations. In this report, the fixed-wing kite of the ground-generating principle is chosen because it is the most used in development. The rated power is assumed to be 500kW. This does not exist yet. However, this seems like a realistic size for the near future. This results in parameters tabulated in Table 2 for the AWE system. The values are based on values from literature [26, 27].



(a) Fixed-wing kite AWE system [24]



(b) Soft wing AWE system [25]

Figure 5: Two wing types in action

Air pressure	ρ	1.2	kg/m^3
Kite area	A_p	45	m^2
Drag coefficient kite	C_D^k	0.067	-
Lift coefficient kite	L	1	-
Drag coefficient tether	C_D^t	1	-
Tether length	r_a	300	m
Tether diameter	d_t	0.025	m
Rated power	P	500	kW
Rated wind velocities	v_w	5 - 25	m/s
Elevation angle	β	30	degrees
Azimuth angle	ϕ	0	degrees

Table 2: Parameters used for Figure 12, from [26, 27]

2.2 Retrofitting offshore wind farms

It is crucial to accurately define the terms used in the context of wind farm upgrades. The term "retrofitting" typically involves replacing certain components, such as the foundation or turbine, with newer, more advanced ones to enhance efficiency and increase power output. On the other hand, "repowering" generally refers to the complete replacement of all parts, including the foundation, while retaining some of the existing infrastructure [28]. Figure 6 shows an example of what a repowered OWF would look like compared to the original OWF. This literature review investigates the option of solely replacing the power-generating components of the wind farm with new technology while reusing the existing foundations and infrastructure. Thus, retrofitting is the appropriate term for this research. The report investigates the replacement of the old OWF with newer larger WTs, including larger foundations for an economic comparison. That would be repowering.

The retrofitting of entire OWFs has not yet been accomplished, largely due to the increased size of wind turbines[8]. W. He et al. [28] discuss the repowering of an OWF, with promising results regarding higher power output, albeit with only partial reuse of the wind farm. This article aims to replace multiple smaller wind turbines with a smaller number of larger ones, which necessitates the removal of the monopiles, as seen in figure 6. This is a costly process and could damage marine life[12, 4]. The initial monopiles must be removed because the larger WTs do not fit on the smaller monopiles.

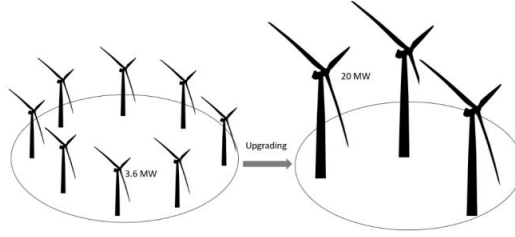


Figure 6: Repowering of WF with new foundations and WTs [28]

A. M. Fowler et al. [4] highlights the positive impact of monopiles on benthic organisms and various fish species, similar to that of offshore platforms, which act as an artificial reef and serve as a habitat for endangered and overfished species. It should be noted that monopiles differ significantly from the offshore platforms mentioned in the paper, as the foundation spacing is vastly different. Nevertheless, the potential positive impact of monopiles is worth noting.

The limited research on the EoL scenarios for wind farms, as noted by A. M. Jadali et al. [29], implies that wind farm operators must devise their own plans for monopile removal, potentially incurring additional expenses. This is confirmed by P. Hou et al. [6] since there are many variables in an OWF, for example, the difference in soil, foundation types, weather conditions, etc. Because of this, other EoL scenarios are discussed in both papers.

According to G. Smith et al. [30], reusing any materials from a decommissioned wind farm, including the foundation, is improbable. It remains unclear from the report whether the reuse of foundations or monopiles is feasible after removal or before. The only exception mentioned is for large concrete gravity-based structures, which may be reused on-site due to the challenges and risks associated with their removal[30]. However, another report by BVG Associates states that recycling an OWF is possible [31]. Only the residual steel value is considered, and the reuse of monopiles in place is not considered. Recycling and reusing are different terms, and both reports agree that reusing is unlikely, while recycling is very well possible.

M. Jadali et al. [29] cited other articles that claimed installing higher capacity wind turbines and modifying key components could extend the operational life of an OWF with minimal additional installation costs. However, G. Smith et al.'s [30] report does not support this claim, nor do the other sources cited discuss the specifics of retrofitting, repowering, or reusing offshore structures. Furthermore, the increase in WT size would make compatibility of the original WTs foundation with the new WTs unrealistic [10, 11]. However, there is one instance where offshore retrofitting was done successfully, backing the statement from M. Jadali et al. [29]. In this project, five offshore 550kW WTs were retrofitted with 660kW WTs[32]. This is only a small increase in rated power. With the larger, modern WTs, repowering is not likely.

Eva Topham et al. [33] discussed the cost and benefits of recycling an OWF during the decommissioning phase, including recycling monopiles. The proposal entails cutting the monopile below the mud line and recycling it for its steel on shore. This is the general approach for decommissioning. Although this article does not discuss reusing or repowering existing offshore infrastructure, it acknowledges the trend towards larger wind turbines requiring larger monopiles[10, 11], making the retrofitting of existing monopiles unlikely.

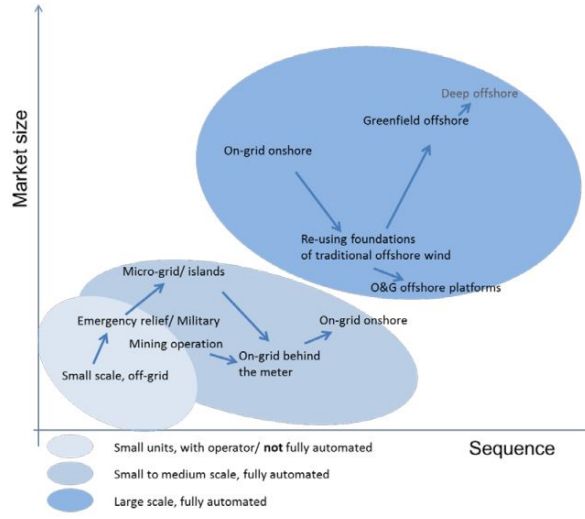


Figure 7: Mentioning of foundation reuse in AWE context [14]

Retrofitting existing monopiles is mentioned in a study by the European Commission [14]. This report explicitly mentions the retrofitting of monopiles with AWE but does not elaborate on it, as can be seen in Figure 7. The report does state that it could be a cost-effective way to penetrate the energy market. In a report by IRENA [34], repowering with AWE is considered a low-risk alternative to showcase the technology. In this report, this is unfortunately also not elaborated on.

Ampyx Power researched AWE at sea[35], with the possible reuse of existing monopiles before their bankruptcy. This research is unfortunately unavailable due to the same bankruptcy. It seems like Ampyx landed on a large-scale floating OWF design with the sea-air-farm project [36]. Retrofitting existing foundations offshore is deemed as a short-term solution by Ampyx [37].

2.3 Foundation analysis

A thorough inspection and assessment of the foundation’s viability for retrofitting is required to retrofit any offshore foundation with a new system. The foundations of offshore wind turbines are an essential component that cannot be replaced without removing other parts, underscoring the importance of inspecting them frequently for potential failure during the lifetime of the OWF[5]. Foundations can experience several failure modes, including fatigue failure[38], cracks and corrosion [39]. To ensure the structure’s integrity, assessing new loads is also crucial.

According to Jadali et al.[29], the wind turbine is the life-limiting factor of an OWF, while other parts have a longer lifespan. The source of this claim is based on current practices, and further research is needed to verify it. However, this should mean that, in many cases, there will be life left in the existing foundations. This chapter discusses the foundation fatigue, the new loads, and the effect of the old loads that still matter.

2.3.1 Fatigue of foundations

Ziegler [40] suggests that if site conditions are less severe than design assumptions, only the fatigue limit state needs to be considered when assessing monopiles. Throughout their operational lifetime, wind tur-

bines experience a range of cyclic loads. According to Sergio M'arquez-Dom'inguez and John D. Sørensen [38], the number of stress cycles per year can be estimated at 3.5E7, which equates to approximately one cycle per second. These cyclic stresses can potentially affect the structural integrity of the monopile.

Fatigue assessment can be performed using various methods. In their study, Sergio M'arquez-Dom'inguez and John D. Sørensen [38] examine several of these methods and investigate the impact of inspections, as well as the lack of inspections, on the lifetime of the structure. One important aspect of inspections is the detection of cracks, as these can significantly affect the fatigue life of a structure. The authors provide a methodology for assessing the fatigue life of a structure based on the observed cracks.

In her work on assessing monopiles for lifetime extension, Lisa Ziegler [41] describes three distinct methods for evaluating the structural reserves of monopiles, which may be viable for lifetime extension. This is particularly relevant to this study, as retrofitting with a new system can be viewed as a lifetime extension. The first assessment method is analytical, followed by data-driven assessment, and finally, practical assessment. Advancements in technology and improved knowledge of site conditions have allowed for more accurate numerical model reruns. On page 15 of her study, Ziegler elaborates on the optimal methods for monitoring fatigue loads, citing multiple sources that have extensively researched this topic. In a case study of an OWF, Ziegler et al. [42] assessed the monopiles using the analytical method. The same approach was applied to the data-driven method in [43] and the practical assessment in [44]. The articles conclude that both data-driven and analytical assessments are viable options for evaluating the structural reserves of a monopile to extend its lifetime and that they can be used in conjunction. However, due to the limited operating window in which a crack may be detected and the system's failure, practical assessment was not feasible [44].

2.3.2 Loads and forces acting on the foundation

The loads acting on the monopile must be evaluated to assess the suitability of existing monopiles for AWE applications. The monopile is subjected to two main loads, wave loads and tether forces, caused by the wind working on the AWE kite. Both loads should be considered. Therefore, the following section is focused on the latter. The section after that is focused on wave-induced loads.

2.3.3 Tether forces due to wind loads

The wind loads are computed for a 500 kW kite system, deemed the most appropriate for this project. As this system is not yet available, the loads must be estimated through calculations or simulations. M. de Lellis et al.[18] provides a formula for determining the power generated by a kite of a particular area, which can be used to estimate the maximum load. This formula for power is the following:

$$P_{cyc} = \frac{C(\alpha) \|\mathbf{W}_{e,r}\|^2 \dot{r}_a \Delta t_{tra} - \|\mathbf{D}_a\| \dot{r}_{a,max} \Delta t_{pas}}{\Delta t_{tra} + \Delta t_{pas}} \quad (1)$$

In this equation, $\|\mathbf{W}_{e,r}\|$ is the effective wind in tether direction. This is specified by

$$\|\mathbf{W}_{e,r}\| = W_n(z) \sin(\theta_L) \cos(\phi_L) - \dot{r}_a \quad (2)$$

Here, $W_n(z)$ is the wind velocity at height z and θ_L is the elevation angle of the tether, and ϕ_L is the azimuth angle of the tether. \dot{r}_a and $\dot{r}_{a,max}$ are the reel-in and maximum reel-in velocity, respectively, Δt_{tra} and Δt_{pas} are the duration of the traction and passive phases. The passive phase is the phase in which the reel-in happens. The traction phase is the electricity-generating phase.

$$C(\alpha) = 0.5\rho AC_L(\alpha)E_{eq}^2(1 + \frac{1}{E_{eq}^2})^{3/2} \quad (3)$$

$C(\alpha)$ is a coefficient that depends on the equivalent aerodynamic efficiency E_{eq} . This equivalent aerodynamic efficiency is the lift coefficient divided by the equivalent drag coefficient, which both depend on α and are kite-specific:

$$E_{eq} = \frac{C_L(\alpha)}{C_{D,eq}(\alpha)} \quad (4)$$

The equivalent drag coefficient $C_{D,eq}(\alpha)$ is not the same as the kite drag coefficient due to the tether drag. This is interesting since the tether drag is often neglected. This results in

$$C_{D,eq}(\alpha) = C_D(\alpha) + \frac{n_c r_a d_c C_{D,c}}{4A} \quad (5)$$

In which n_c is the number of tethers, r_a is the distance between the ground station and the kite, d_c is the tether diameter and $C_{D,c}$ is the drag coefficient for the tether. According to this equation, the tether drag increases with diameter, length and drag coefficient, decreasing with an increase in kite area. This means that with a substantially larger kite and smaller tether, the drag of the tether could indeed be neglected. However, as the flight height increases, the tether will become longer and have a larger diameter.

This equation by M. de Lellis gives the power generation over the entire cycle: Power generation and reeling in. The maximum tether force will be reached during the traction phase. The power generation during the traction phase can be approximated by

$$P_{tra} \approx C(\alpha) \|\mathbf{W}_{e,r}\|^2 \dot{r}_a \quad (6)$$

The maximum tether force can then be calculated with

$$T = \frac{P_{tra}}{\dot{r}_a} \quad (7)$$

If the equation for the power generation during the traction phase is then substituted in the equation for the tether force, then this results in the following equation:

$$T_{max} \approx C(\alpha) \|\mathbf{W}_{e,r}\|^2 \quad (8)$$

This equation takes the tether drag and angle into account through $C(\alpha)$ and $\|\mathbf{W}_{e,r}\|$ and looks like this when everything is substituted:

$$T_{max} \approx C(\alpha) \|W_n(z) \sin(\theta_L) \cos(\phi_L) - \dot{r}_a\|^2 \quad (9)$$

M. de Lellis also recommend the maximum tether velocity as a limiting factor and optimizes around it by limiting the reel-in and reel-out velocity.

U. Fechner and R. Schmehl [26] provide a formula for the maximum tether force as well, which is similar to the equation of M. de Lellis:

$$F_{t,max} = \frac{1}{2} \rho v_a^2 A_p C_D \sqrt{1 + (\frac{L}{D})^2} \quad (10)$$

In this equation $v_a = (v_w \cos \beta \cos \phi - r_a) \sqrt{1 + (\frac{L}{D})^2}$, which is essentially the same as the formula for $\mathbf{W}_{e,r}$, only the angle is taken with respect to the ground instead of the vertical axis. The added root compensates in the equation. The drag is calculated with

$$C_D = C_D^k + 0.31 r_a d_t C_D^t \frac{1}{A} \quad (11)$$

This is the same equation for drag given by M. de Lellis. Only here, 0.31 is used instead of 0.25. In [26], more comprehensive reasoning is used for this value, and the complete equation is clearer. Therefore, the equation by Fechner and Schmehl [26] will be used, even though they are essentially the same.

The tether force that results from this formula can be plotted against the apparent wind velocities. The apparent wind velocities, however, depend on the wind velocity and the reel-out velocity. Since there is a maximum to the tether loads and the fact that the reeling speed can be controlled and the wind velocity cannot, the plot in figure 8a is only dependent on the reel-out speed and the wind velocity is fixed at 10 m/s. The parameters used are provided in table 2.

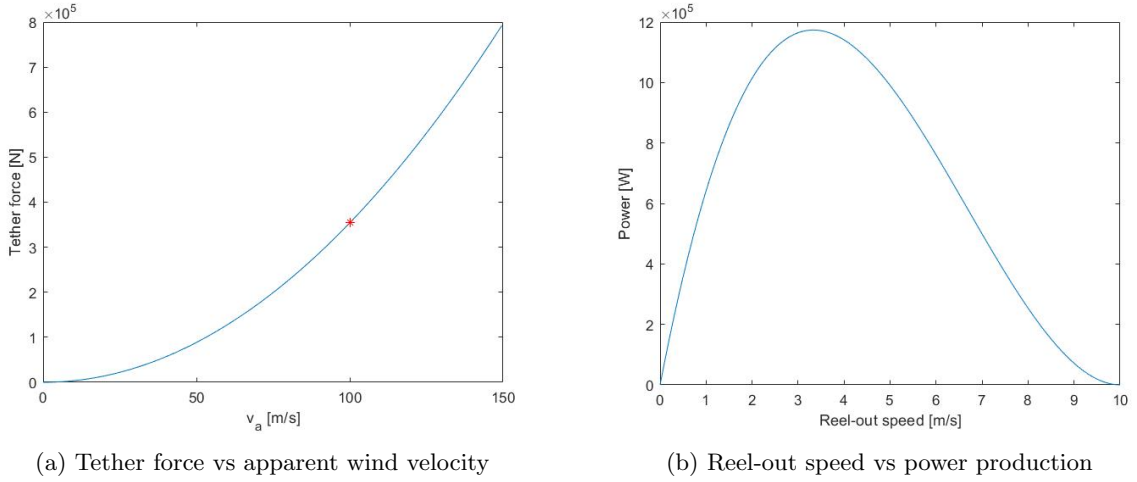


Figure 8

In this graph, the apparent wind velocity is very high, and as a result, the maximum tether force is also very high. This high apparent wind and tether force results when the kite is not being reeled out. Since power production would be zero, that would be unlikely. In the graph in figure 8b below, the reel-out speed is plotted against power. This shows a most efficient reel-out speed of 3.3 m/s. If this value is substituted in equation (10), a tether force of 355kN is obtained. This is well below the maximum tether force of 56.9 tons that De Lellis used in [18]. It should be noted that this is the maximum tether force at optimal power production. However, this tether force can be limited by varying the reel-out speed and changing lift and drag ratios on the kite. This could be necessary to keep the horizontal loads on the monopiles small.

Although the maximum wind loads are significant, the fatigue loads are more critical since the site conditions are less severe than the design assumptions [40]. A detailed flight path is necessary to calculate the fatigue loads, including apparent velocities. However, Fechner and Schmehls [26] formula only provides the maximum tether force. A more intricate system is needed for the calculation of all aerodynamic loads. To achieve this, a numerical model should be used. This could produce a load curve that must

be compared to the foundation's design loads. The largest tested AWE system is the Makani M600 [45], which utilizes onboard power production instead of ground power production. The kite flies crosswind in loops, implying that the tether forces may be in the same order of magnitude. However, this cannot be controlled with the reel-out speed. Thus, some differences should be noted. The tether on this system could withstand a force of 250 kN [46]. The safety margin for AWE tethers is 3 [47], so this system was built for a maximum tether force of 83.3 kN. This force acts at an angle thoroughly documented in various literature as it directly affects efficiency [26]. A simple calculation shows that this force is a fraction of the horizontal force on a wind turbine with the same power output. Furthermore, the absence of a tall tower needed for a wind turbine results in a smaller overturning moment because the tower is shorter. Although this observation appears promising at first glance, further investigation is required to verify the effect and amplitude of fatigue loading caused by the wind loads of the AWE system.

2.3.4 Wave loads

For AWE on monopiles, the wave loads are probably the more significant loads, primarily because the system does not require a large tower. As a result, the overturning moment generated by the wind on the monopiles is much less than conventional wind turbines. As shown in the previous section, the maximum tether force by a 500kW kite is 355kN. In another paper, M. de Lellis et al. [21] provide an equation for the horizontal thrust force acting on a wind turbine:

$$F_{thrust} = \frac{1}{2}\rho A_2 U_w^2 4a(1-a) \quad (12)$$

In this equation, A is the swept area of the turbine, U_w is the wind velocity without obstruction, and a is the axial induction factor. The upper limit of this factor is $\frac{1}{2}$ and the optimal value for a is $\frac{1}{3}$. For this calculation, the optimal value is chosen. Table 1 shows that most wind turbines relevant for this study are in the 2MW range. Therefore, the swept area is calculated with

$$P = \frac{1}{2}\rho A U_w^3 4a(1-a)^2 \quad (13)$$

With P is 2MW, U is the rated wind velocity, in this case, taken to be 12m/s. This results in a swept area of $416.7m^2$ and thus a rotor length of $32m$. With these values substituted in equation 12, a value of 250kN is obtained at the rated wind velocity. With the significantly longer tower needed for a WT, the overturning moment will be substantially larger for the WT than for the AWE system. This highlights the need to consider the wave loads on the monopiles properly.

Wave loads and their effects on monopiles are researched extensively. For example, Ziegler et al. [48] present a method to calculate wave-induced fatigue loads. This study showed to have over 90% accuracy compared with a real-world case study. According to this study, the most important factors were the water depth and wave period. This study states that the method is mostly viable for preliminary design and support structure optimization, which could be used to determine the ability of monopiles to withstand wave loads for 20 more years. The method is a frequency-domain analysis of the monopiles and can assess the wave-induced fatigue damage. The method is based on a linearised Morison equation for wave loading. Then, the internal loads are derived from a finite element (FE) model. Lastly, equivalent load ranges are obtained from the response spectra. This results in an output of equivalent fatigue loads (EFL) for a specified number of cycles, which could be used to determine the structural integrity of the monopile. it is important to note that for a frequency domain analysis, the necessary data is vast and might be difficult to obtain. Other methods, therefore, might be preferred for this research.

Vorpahl et al. [49] studied several loads on offshore wind turbines and how to design accordingly. This includes wave loads, and they describe how calculations can be done with these wave loads. They also give

an extensive list of calculation tools to calculate the hydrostatic and dynamic loads on the foundations accurately. Their study makes a statement about the massive overestimation that occurs when simulations are not done carefully and the structural reserves that result from that. In the first stages of offshore wind, there were a lot of uncertainties. As a result, the foundations were overdesigned. Therefore, for some retrofitting activities, the foundations do not have to be looked at, especially concrete foundations [6].

According to Seidel [50], the wave-induced fatigue loads are determinative for the calculations of the monopile. He also says that a quick way to calculate fatigue loads can be derived with relatively uncomplicated formulas and simplifications. Seidel does this with simplifications and calculations in the frequency domain. Ziegler et al. [48] did that as well. When the calculations in the frequency domain are impossible due to a lack of data, the structural reserves can be calculated with SN curves and measured or assumed data over the past years. This opposes the earlier statements that it is very complex to do such things. If possible, both should be done and compared to get a good result. Yeter and Garbatov [51] provide extensive research, including several models to assess a support structure's remaining lifetime. They also made a risk-based framework to assess the structural integrity of a structure. This can be used to predict the lifetime of structures as well. Yeter and Garbatov [51] also provide an assessment for structural integrity using SN curves. This approach only works, however, if the structures are intact. For structures with cracks, a fracture mechanics approach should be used. For this research, the method with SN curves and measured or assumed data is used, due to the lack of real data near the considered OWFs.

2.4 Economics

The economics of retrofitting an OWF with an AWES is essential. Since this has not yet been done, a general economic picture of AWE is made, and a comparison has been made to lifetime extension and the cost savings that can be made by doing such a thing. Furthermore, the important economic factors are discussed.

2.4.1 Economics of AWE

A fair amount of literature is available about the economics of AWE. Heilmann and Houle [52] introduce the economic assessment of an AWE system. They consider site and system characteristics as influence factors, among other things. For this research, both the site and system are fixed, and for the site specifically, there should be a lot of data gathered over the years the original wind farm was operating. This data will consist of predictions and assumptions that AWE companies should provide for the system. The most important site characteristic is the wind velocity at operating height. For the system, the most important characteristic is the power curve. The relevant factors for the power curve are discussed in section 2.3.3. However, there are other important factors to consider for the power curve, such as the elevation angle, the height of the kite and the azimuth angle. The same article provides a table of the initial investment cost. This table is visible in figure 9 below.

Heilman and Houle [52] discuss the cost of scaling. They find that the cost of the generator scales with power and force as follows:

$$Cost_{generator} \sim \sqrt{P_o} F^{3/4} \quad (14)$$

This is important to consider since the 500kW system does not exist yet. Scaling costs like this could provide a general idea of the economics of the system.

Component Group	PKG	Conv. WT	Main Cost Driver
1 Wind capturing device	Kite	Rotor blades	Span or area
2 Mech. power conversion	Winch, generator, (gearbox)	Generator, (gearbox)	Force and power capabilities
3 Supporting structure	Tether	Tower	Length of structure and applied forces
4 Electr. power conversion	Inverter, transformer, (storage)	Inverter, transformer	Power capabilities
5 Balance-of-station	Transport, installation, etc.		System size and complexity

Figure 9: General categorisation of costs of AWE system vs WT

According to Ellis et al. in [18], the capacitor factor for AWE is higher than for conventional wind energy. This is good news for the economics of AWE, as it results in a potentially higher energy yield. In this paper, however, the numbers for AWE might be slightly exaggerated because they make assumptions favouring AWE. For further economic analysis, they calculate several costs, for example, the cost of the kite. For the breakdown of these costs, they refer to the master thesis of Heilmann [53], who has developed a method for this. This method, however, only considers soft-wing kites. To analyse the cost of AWE, a framework provided by the UN can be used [54]. In a report by BVG associates [55], economic aspects of onshore and offshore AWE systems are discussed as well. This report also emphasises the size of offshore AWE, where a larger system is likely to be more profitable.

2.4.2 Cost of retrofitting

Retrofitting with a new system comes at a cost, but there are also several savings. This section discusses the prices and savings with literature and which factors are essential. For the actual retrofitting, the cost of the kites, the installation cost, and the maintenance of both the kite system and the foundation are important. The installation cost includes the cost of modification of the monopiles. This can be estimated with information from [31] and [54]. The former gives estimations of prices for installing entire wind farms, while the latter estimates costs for the modifications, considering the amount of work and steel. The price for installing OWFs is largely based on component costs and vessel day rates. Especially for the latter, the time it takes to install an OWF is crucial. Reducing installation time immediately reduces the cost of an OWF. The same holds for the removal and retrofitting of an OWF.

2.4.3 Maintenance

Another important factor that needs to be considered is that the AWE system needs to be maintained. Economic analysis and breakdown of the different options can be done. Conventional OWFs have between 3% and 18% of the total lifetime costs assigned to operation and maintenance [56, 31]. A comparison to this number should be made and ideally would be lower for AWE. BVG associates published a guide to OWF[31], with a total cost breakdown of everything needed to build an OWF. This guide closely examines maintenance, separating it into different parts. For maintenance, a distinguishment is made for turbine and balance of plant maintenance. The maintenance of the balance of plant (BoP) includes maintenance to and inspection of the foundation, cables, substation and scour, as well as the remotely controlled vehicles used to do inspection underwater. According to [31], the cost of maintenance and operation of the foundations of an OWF is only a fraction of the total cost of an OWF: €48 million in operation and maintenance of the foundations and a total OWF cost of €2000 million. It should be noted that the OWF in this report is 1GW, and scaling is not linear, but it will give an indication of maintenance cost to the foundation.

2.4.4 Market factors

A crucial part of the economics is the market environment. This will determine whether or not a project is feasible [52]. The electricity prices for renewable energy in Europe are essential since that will create revenue. Furthermore, initial investment is needed. Several economic indicators can be used to secure such investment to assess the financial feasibility.

2.4.5 Levelized cost of energy

The levelized cost of energy (LCoE) measures the cost of energy per unit produced. All the costs and energy flows are discounted. The costs are divided into initial investment, operation and management, and decommissioning. That results in the following equation:

$$LCOE = \frac{\sum_{t=0}^T \frac{I}{(1+r)^t} + \frac{O}{(1+r)^t} + \frac{D}{(1+r)^t}}{\sum_{t=0}^T \frac{E_t}{(1+r)^t}} \quad (15)$$

In this equation, I is the initial investment, O are the operation and management costs, D is the cost of decommissioning, E_t is the annual energy production, r is the discount rate, and T is the total lifetime of the system. With the LCoE, the system can be compared to other systems fairly, independent of local energy tariffs. In figure 10, the I, O and D are broken down for a conventional OWF [57].

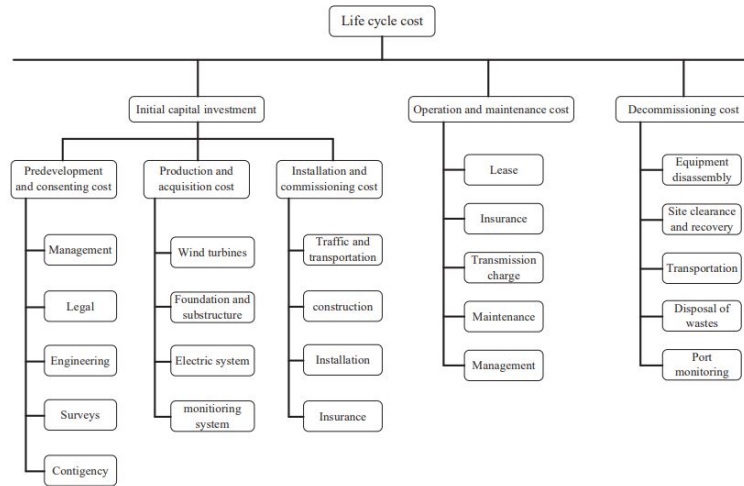


Figure 10: Cost composition of OWF

Values for the LCoE in literature are €137/MWh [36] for a floating offshore AWE wind farm. In the calculation for this LCoE, however, the CAPEX is covered for 50% by the floaters and mooring system. Therefore, the floaters have a significant role in this LCoE. In a report by BVG associates [55], the LCoE for onshore AWE wind farms in 2030 is calculated to be over €60/MWh. This is significantly lower than the €137/MWh earlier, as expected, since it lacks the offshore foundations. An LCoE for conventional OWFs is given by [58]. This report states an LCoE of €100/MWh for conventional WTs offshore in 2015. This value has dropped significantly to €50/MWh in 2022. NREL has a review on the cost of wind energy. In this report, an LCoE of €85/MWh is given for bottom-fixed offshore wind energy [78]. Values for discount rates vary as well. In the same NREL [78], a discount rate between 3.76% and 6.26% is given. BVG Associates give a discount rate of 6% in [31].

2.4.6 NPV

Another important economic indicator is the net present value (NPV)[57]. The NPV is the sum of all the costs and income, divided by a discount rate and often a factor for inflation. That results in the following equation:

$$NPV = \frac{\sum_{t=1}^T -I - O + E_t * C}{(1 + r)^t} \quad (16)$$

In this equation, C is the cost of energy E_t per MWh. I is the initial investment and O are the cost for operations and maintenance. The discount rate is given by r and is taken conservatively with 0.07.

2.5 Research question

This literature review discovered a knowledge gap and a research question was formulated. This report aims to answer the research question and subquestions that are stated as follows:

Is installing airborne wind energy systems on the monopiles of decommissioned offshore wind farms structurally and economically viable?

To answer this research question, the following subquestions must be answered.

1. What are the dominant loads, and how can the expected lifetime of the foundations be calculated?
2. Is retrofitting offshore foundations economically feasible?
3. What are the alternatives for retrofitting with AWE, and can that be more feasible than retrofitting with AWE?

To answer these questions, this report is structured as follows. First, the principles of AWE systems are briefly discussed. Secondly, the loads on foundations and their consequences on the lifetime of the foundations are determined. This is done by analysing the loads and stresses on the foundations in two existing OWFs, Nysted and Horns Rev I, details of which are provided in Table 1. Thirdly, two options to optimize the system are determined and analysed for their structural feasibility. The economics of the AWE systems on used foundations are discussed in the next chapter. This is done by analysing the revenue and costs of retrofitting offshore foundations with AWE systems in OWF settings. A competitive alternative is provided as well to make a fair comparison. In Section 6, economic optimizations are discussed, followed by recommendations in Section 7. In the last chapter, a conclusion is drawn.

3 Structural Reserves in Foundations

To retrofit existing offshore structures with AWE systems, the structures must possess sufficient structural reserve to sustain operation for at least another 25 years. Assessing structural reserves in the foundation requires a thorough understanding of the loads acting on the structure. In this section, these loads are calculated and compared to the original loads to determine compliance with the ultimate limit state (ULS). Additionally, load ranges are determined, from which stress ranges are derived. A fatigue analysis is then conducted to ascertain the fatigue limit state (FLS) and estimate the remaining fatigue lifetime of the structures. If the structure can withstand both ULS and FLS, it becomes a viable candidate for retrofitting with AWE systems.

3.1 Loads

The primary loads acting on the foundations consist of wind and wave loads. This section calculates the loads for a specific type of AWE system and evaluates them for two different foundation types: a concrete gravity-based structure and a monopile. The parameters of the two types of structures are based on the OWFs of Nysted (GBS) and Horns Rev I (Monopile). Wind loads are represented as tether loads arising from the wind's action on the kite. This approach is best illustrated through Figure 11.

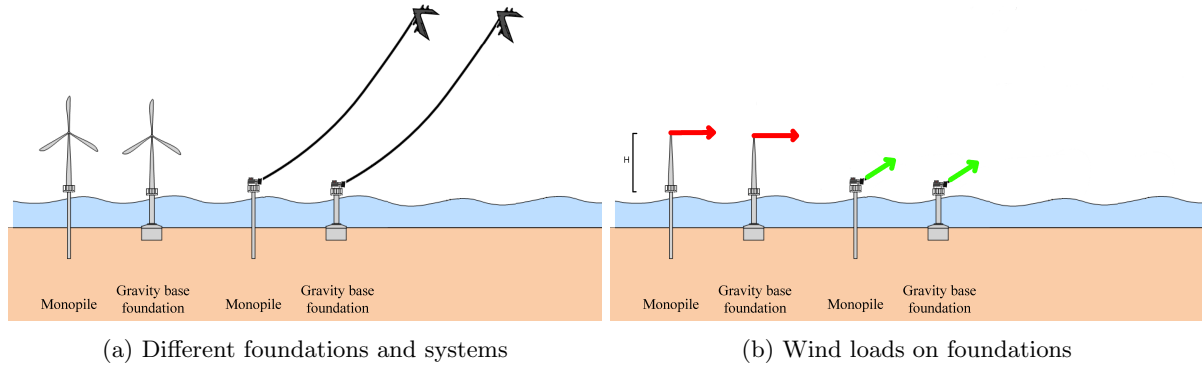


Figure 11: Foundations, systems and loads

3.1.1 Tether loads

As discussed in the previous section, only one AWE system is considered: a 500kW rigid-wing kite with values based on literature (see Table 2 in Section 2.1). For a rated power of 500kW, the peak power of the AWE system must be higher to take the losses during reel-in into account. Therefore, for the calculations on tether loads, a factor of 1.5 is used over the rated power, resulting in a peak power of 750kW. With these inputs, the maximum tether forces can be calculated. The tether force depends, among other things, on the reel-out velocity of the tether; the faster the tether is reeled out, the less force it experiences ('letting go' of the kite). The tether force is computed using the following equation from [26]:

$$F_{t,max} = \frac{1}{2} \rho v_a^2 A_p C_D \sqrt{1 + \left(\frac{L}{D}\right)^2} \quad (17)$$

In this equation, the apparent wind velocity is denoted by

$$v_a = (v_w \cos \beta \cos \phi - \dot{r}_a) \sqrt{1 + \left(\frac{L}{D}\right)^2} \quad (18)$$

Here, v_w represents the wind velocity at the operational altitude of the kite, and \dot{r}_a denotes the reel-out velocity. The elevation angle of the kite with the ground is given by β , and the azimuth angle is given by ϕ . L and D are the lift and drag coefficients of the kite, and the combined drag coefficient C_D can be calculated with:

$$C_D = C_D^k + 0.31 r_a d_t C_D^t \frac{1}{A} \quad (19)$$

This drag equation consists of two parts: the drag of the kite and the tether drag. The tether drag is multiplied by 0.31 as it experiences varying velocities along its length[26].

From the equation of the tether force, the output power can be calculated with:

$$P_{trac} = F_{t,max} \dot{r}_a \quad (20)$$

Both the tether force and power output depend on the reel-out velocity. This allows optimising and plotting the tether force against power for a specific wind velocity. That results in the graph in Figure 12.

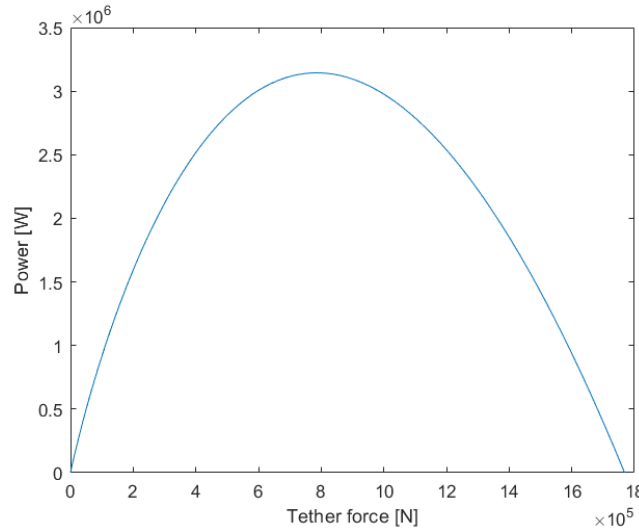


Figure 12: Tether force vs power at 12 m/s wind velocity. Other parameters can be found in Table 2

The maximum power output reached 3.14MW, exceeding this system's peak power of 750kW. The peak output power is limited to 750kW to ensure practical operation, resulting in a tether force of 79.2kN. The rated power of the system is 500kW, and the peak power of 750kW compensates for the reel-in phase since it is a pumping system. The output power can be limited by adjusting the reel-out velocity for various wind velocities. However, this poses a challenge, as the system will not reach its maximum power output of 750 kW for lower wind velocities. Therefore, the maximum power output with the corresponding tether forces should be considered for lower wind velocities. As a result, the tether forces

are high in wind ranges that produce a power output close to 750kW. Figure 13 displays the theoretical tether forces of this 750kW system, optimised for the maximum power, taking the elevation angle of 30 degrees into account. The elevation angle of 30 degrees results in higher tether forces than a zero-degree elevation angle.

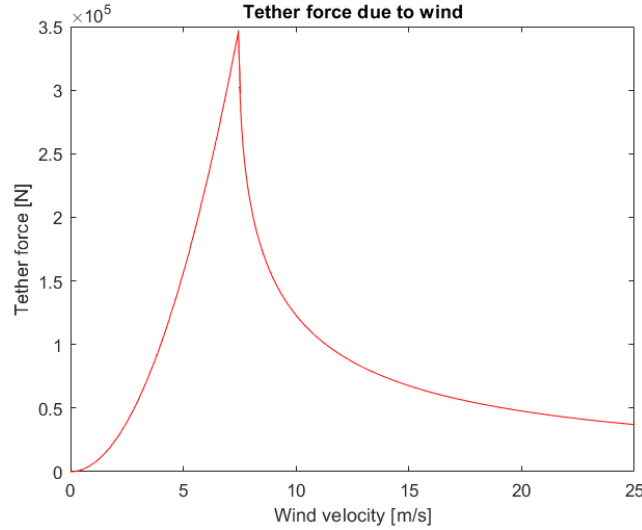


Figure 13: Maximum tether forces due to wind for the full wind range

The maximum tether force, in this case, is 347kN at a wind velocity of 7.45 m/s. However, such a large force is unrealistic for a tether to withstand. A Dyneema tether, for example, can withstand 1073N/mm^2 [26]. Since tether drag and weight impact the efficiency and cost of the AWE system, it is crucial to consider this. To withstand the calculated load of 347kN, a tether with a diameter of 35 mm is needed, considering a safety factor of 3.0. A more realistic tether diameter would be 25 mm, resulting in the graph shown in Figure 14, where the peak is flattened to accommodate the limited force on the tether.

This limitation results in a different power output curve, where the maximum power of 750kW is reached at a higher wind velocity, as shown in Figure 15. The less steep power curve may yield lower yearly power generation, depending on the location and wind characteristics.

For the calculations on the foundations, the wind loads are crucial. In this section, the tether loads due to wind are calculated. The maximum tether force on the foundation is 347kN for an unlimited tether diameter with a 750kW maximum power AWE system and the kite flying at an elevation angle of 30 degrees. However, if the tether diameter is limited to 25mm, the maximum tether force is reduced to 176kN at an elevation angle of 30 degrees. For the foundation calculations, the latter tether force will be used.

The tether loads due to wind are not constant at the maximum force. During the reel-in phase, the force is lower; during the reel-out phase, the tether force is subject to fluctuations. These fluctuations arise due to the influence of gravity on the kite's motion when flying in a lying Figure eight pattern. As the kite goes up and down twice per entire loop, gravity causes variations in its speed: it accelerates when descending and decelerates when ascending. Consequently, this leads to larger apparent wind velocities

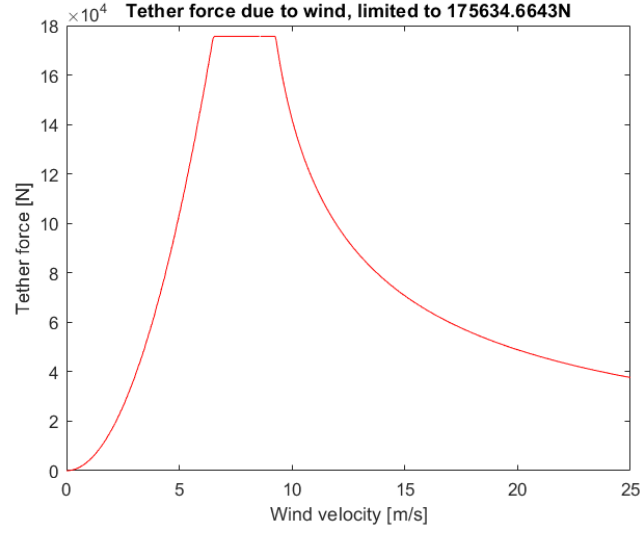


Figure 14: Maximum tether forces due to wind for the full wind range, limited for a 25mm tether

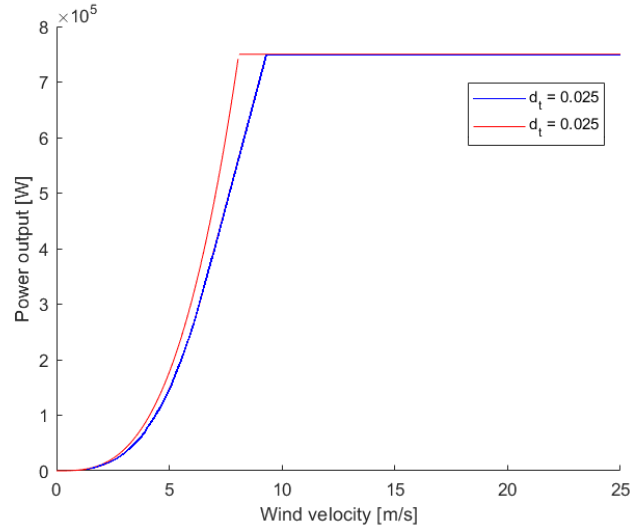


Figure 15: Power curves for a tether diameter of 25mm and 35mm. Steeper for 35mm

during the downward movement and smaller apparent wind velocities during the upward movement. Equation 17 highlights the substantial impact of this apparent wind velocity variation on the tether force due to wind.

The accurate description of the kite's flight path falls beyond the scope of this research; hence, a different approach is adopted to model the effect of gravity on the tether loads. The analysis considers a maximum tether force of 176kN, chosen because it corresponds to the tether force in the wind range of 5.5 to 8.7m/s, the most common wind range in Nysted and Horns Rev I. A sine wave with a specific

amplitude and period is added to the maximum tether force to account for the effect of gravity-induced fluctuations. The amplitude is assumed to be a constant percentage (20%) of the maximum tether force based on comparisons with actual flight data of a smaller kite [27].

Considering the kite's flight radius of 64 m (according to [27]), its velocity at a wind speed of 8m/s, and the fact that the kite completes two full loops during its motion, the period is calculated to be 6.5s. The duration of the reel-out phase can be determined by dividing the length of the tether reeled out by the reel-out velocity, using the reel-out velocity at a wind speed of 8m/s. A reel-in velocity of 8m/s is applied for the reel-in phase. This is based on the value from [18]. During the reel-in phase, the lift coefficient of the kite is lowered to ensure a smooth return of the kite with minimal energy loss. The lift coefficient is reduced to 0 for the calculations in this report, although this is not feasible in practice. However, this conservative approach allows for a broader range of loading, as utilised in Section 3.3 for fatigue calculations.

Accounting for the force fluctuations due to gravity while reeling out and the force difference between the reel-out and reel-in phases results in a time-dependent tether force profile. This is illustrated in Figure 16. The minimum tether force during the reel-out phase is 141kN, and the maximum during the reel-out phase is 211kN. In contrast, the force during the reel-in phase is 816N, which is considerably lower, as previously explained.

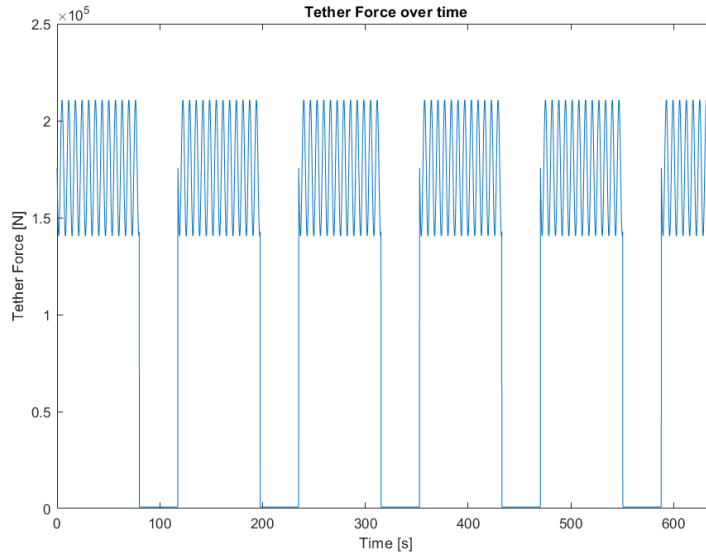


Figure 16: Fluctuating tether force due to gravity ($T = 6.5\text{s}$) and difference between reel-in and reel-out ($T = 117\text{s}$)

3.1.2 Wave loads

Installing an AWE system does not alter the wave loads on the foundation. Nevertheless, it remains crucial to account for these wave loads in the calculations concerning the expected lifetime of the AWE system. To calculate wave loads, specific parameters are required, including the wave height, water depth,

wave period, and foundation diameter. These parameters are location-specific and not publicly available. Therefore, the wave loads are calculated for two existing OWFs suitable for retrofitting with AWE and a reference OWF with conservative parameters.

The wave loads are calculated with the Morison equation. The Morison equation consists of a drag part and an inertia part and is given by Equation 21.

$$f(z) = f_d(z) + f_i(z) = \frac{1}{2}\rho C_D Du(z)|u(z)| + \frac{\pi}{4}\rho C_M D^2 \dot{u}(z) \quad (21)$$

In this equation, $f(z)$ is the wave force at height z , where $z = 0$ at the mean sea level (MSL). The drag part of the equations is given by $f_d(z)$, and the inertia part is given by $f_i(z)$. The water density is given by ρ . The drag coefficient and inertia coefficient are given by C_D and C_M , respectively. These are calculated conservatively from DNVGL standard ST-0437 [59], at 1.9 and 2.0, respectively. The foundation diameter is given by D . Lastly, the water particle velocity, $u(z)$, and acceleration, $\dot{u}(z)$, are described by Airy wave theory with Equations 22 and 23.

$$u(x, z; t) = \zeta_a \omega e^{kz} \cos(kx - \omega t) \quad (22)$$

$$\dot{u}(x, z; t) = \zeta_a \omega^2 e^{kz} \sin(kx - \omega t) \quad (23)$$

In these equations, ζ_a is the wave amplitude, ω is the wave frequency, k is the wave number and x is the location of the water particles with respect to the foundation. For these calculations, x is taken as zero. For this report, only the maximum and minimum values for the wave loads are of interest. To obtain the maximum value for $f_d(z)$, the maximum value for $u(x, z; t)$ is needed. Therefore, the maximum water particle velocity $u_{max}(z) = \zeta_a \omega e^{kz}$ is used. To obtain this maximum water particle velocity, $\cos(kx - \omega t)$ is substituted with 1. For the minimum value, it must be replaced with -1. The same can be done for the maximum water particle acceleration needed for the maximum value of $f_i(z)$: $\dot{u}_{max}(z) = \zeta_a \omega^2 e^{kz}$. In both instances, ζ_a can be replaced with $\sqrt{H_s^2/8}$, as described at the beginning of this section.

To obtain the total maximum value of the wave loads, Equation 21 must be integrated over z . This will result in the maximum base shear of the foundation. The maximum overturning moment can be obtained by multiplying $f(z)$ with $(d - z)$ and then integrate over z , where d is the water depth. The result is Equation 24 for the maximum base shear and Equation 25 for the maximum overturning moment.

$$F_{base} = \int_{-d}^0 f(z) dz \quad (24)$$

$$M_{overturning} = \int_{-d}^0 f(z)(d + z) dz \quad (25)$$

Specific parameters are required to calculate the actual wave loads on the foundations. Table 3 summarises the water depth, foundation diameter, significant wave height, and period for three locations: Nysted, Horns Rev I, and a reference OWF. The reference OWF is a fictional OWF with parameters chosen to ensure a very conservative outcome. As the wave height and period data are not publicly available for these locations, data from buoys near the OWFs, specifically Zingst near Nysted and Westerland near Horns Rev I, is utilised [23]. The mean and median significant wave heights over 12 years for these locations were available, and their averages are employed as validation for the calculations used to obtain the significant wave heights and periods in this study. These are, therefore, the most common wave heights and not the maximum wave heights over the 12 years it was measured. The locations of the



Figure 17: Wave buoy (Westerland and Zingst) locations for calculation verification

considered OWFs and the closest wave buoys with public data are visible in the map in Figure 17. The calculations are based on the theory for modelling waves in coastal waters. The method can be found in Equation 26 - 30. The parameters are in the formula sheets in Appendix B. While it is important to note that this data may not be entirely accurate, OWF owners usually possess private data from their own wave buoys and weather stations, enabling them to obtain more precise wave heights for more accurate wave load calculations.

$$H_{m0} = \frac{\tilde{H}_{m0} * U_{10}^2}{g} \quad (26)$$

and

$$T_{m0} = \frac{\tilde{T}_{m0} * U_{10}}{g} \quad (27)$$

Here, \tilde{H}_{m0} and \tilde{T}_{m0} are the dimensionless significant wave height and period, respectively. They are calculated with the equations below. U_{10} is the wind velocity 10m above sea level.

$$\tilde{H}_{m0} = \tilde{H}_{\infty} \left[\tanh \left(k_1 \tilde{F}^{m_1} \right) \right]^p \quad (28)$$

and

$$\tilde{T}_{m0} = \tilde{T}_{\infty} \left[\tanh \left(k_2 \tilde{F}^{m_2} \right) \right]^q \quad (29)$$

Here, \tilde{F} is the dimensionless fetch, which is calculated with the following equation from the fetch F , or distance to shore in the prevalent wind direction and k_1, k_2, m_1, m_2, p and q are constants.

$$F = \frac{\tilde{F} * U_{10}^2}{g} \quad (30)$$

The calculated data in Table 3 exhibits close agreement with the measured data obtained from nearby locations. Consequently, for this research, the calculated data is considered more accurate, considering the distances between the wave buoys and the OWFs. The measured data verifies that the computed data falls within the correct order of magnitude, thereby ensuring the reliability of subsequent calculations. However, it is essential to acknowledge that if an OWF owner contemplates retrofitting with AWE, they must conduct these calculations using their specific data, as OWFs vary significantly in terms of environmental conditions and dimensions.

Table 3 provides an overview of the calculation parameters and verification results for the three locations: Nysted, Horns Rev I, and a reference OWF. The foundation diameter, water depth, and the measured and calculated significant wave height and period are recorded. The measured values for H_s and T_s at Nysted and Horns Rev I were 0.68m, 3.6s and 0.88m, 5.6s, respectively. The calculated values for H_s and T_s at these locations were found to be 0.63m, 3.3s and 1.0m, 5.0s, respectively. For the reference OWF location, where measured data was unavailable, the calculated significant wave height and period were 1.5m and 7.0s, respectively.

Location	Foundation diameter	Water depth	H_s measured	T_s measured	H_s calc	T_s calc
Nysted	4.08 m	9m	0.68m	3.6s	0.63m	3.3s
Horns Rev I	4.2m	14m	0.88m	5.6s	1.0m	5.0s
Reference OWF	4.0m	16m	-	-	1.5m	7.0s

Table 3: Calculation parameters and verification

3.1.3 Wave load results

The wave force on the foundations is evaluated using the parameters derived from the previous section and summarised in Table 3. By employing Equation 24 and filling in the parameters from the different locations, the maximum base shear can be calculated. For Nysted, the result was a base shear due to wave loads of 57.3kN. For Horns Rev I, this was higher with a base shear as a result of wave loads of 89.3kN, and for the reference OWF this was 106kN. The differences in wave forces for the different locations are caused by the different wave heights. The water depth, foundation diameter, and wave period have an influence on the total wave force as well. However, this is to a lesser extent. The wave force is not acting in one point but is distributed over the length of the foundation. This is visualised in Figure 18a for Nysted. In this figure, the different parts of the Morison equation are split. The influence of the drag part of the Morison equation is small in comparison with the inertia part of the equation, which can also be seen in Figure 18b. Notably, the graph represents a regular wave, implying that the structure is cyclically loaded. While this may not hold for irregular waves present in the sea state, the realistic values for significant wave height and period used in the calculations accurately estimate the order of magnitude and frequency of the structure's load over a more extended period. This information is crucial for the fatigue and lifetime calculations conducted in Section 3.3.

Due to how the wave force on the foundation is distributed, the overturning moment cannot be calculated by multiplying the water depth by the total wave force. Instead, Equation 25 must be used. This results in an overturning moment caused by waves of 381kNm for Nysted, 850kNm for Horns Rev I and 1.06MNm for the reference OWF. Wheeler stretching is applied to account for the waves above MSL. As a result, the graphs in Figure 18a go above $z = 0$ since the waves go above $z = 0$ as well. All the results

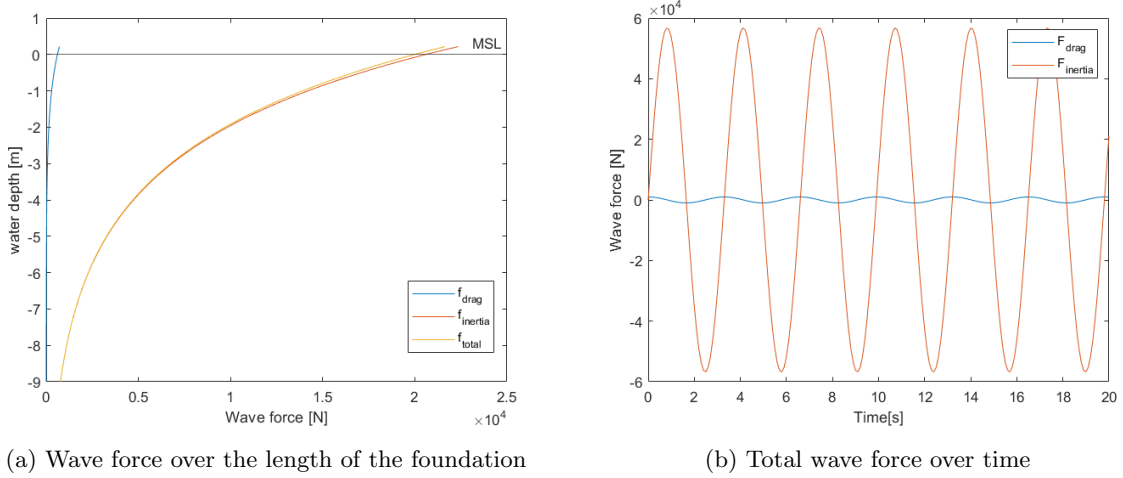


Figure 18: Wave force at Nysted

are summarised in Table 4.

	Max force	Min force	Force range	Overturning moment	Wave height	Period
Nysted	58.9kN	-58.9kN	117.8kN	393kNm	0.63m	3.3s
Horns Rev I	90.3kN	-90.3kN	180.6kN	852kNm	1.0m	5.0s
Reference OWF	106kN	-106kN	212kN	1.06MNm	1.5m	7.0s

Table 4: Summary of the wave forces and moments on the different foundations, acting at the seabed

3.2 ULS

To assess whether the installation of an AWE system exceeds the ULS, a comparison between the base shear and overturning moment caused by the system and the original WTs is essential. Specifically, the axial force over the wind range for the original WTs is required to make this comparison. With the axial force information, the base shear can be readily calculated, and by knowing the length of the original tower and foundation, the overturning moment can also be determined. For Nysted, the rated power of the WTs is 2.3MW with a rotor radius of 41.2 m, while at Horns Rev I, the rated power is 2MW with a rotor radius of 40.0 m. Unfortunately, there is insufficient publicly available data to calculate the horizontal axis force of these WTs directly. As an alternative approach, the thrust force of a rotor can be computed using the equation:

$$F_{thrust} = \frac{1}{2} \rho_{air} A v_w^2 4a(1-a) \quad (31)$$

In this equation, A represents the swept area of the rotor, and a is the axial induction factor, which is limited to $\frac{1}{2}$. Unfortunately, the value for a is unknown, but there is a way to calculate it with the information at hand. The power of a WT is given by

$$P_{wt} = \frac{1}{2} \rho_{air} A v_w^3 4a(1-a)^2 \quad (32)$$

Using the provided power curve for the WT at Nysted (Figure 19a[60]), the power outputs at various wind velocities are known. By solving for a for each wind velocity, this value can then be substituted into Equation 31, resulting in a thrust force graph, as shown in Figure 19b. The maximum thrust force, and thus the maximum horizontal force for the WTs at Nysted, is calculated to be 189 kN.

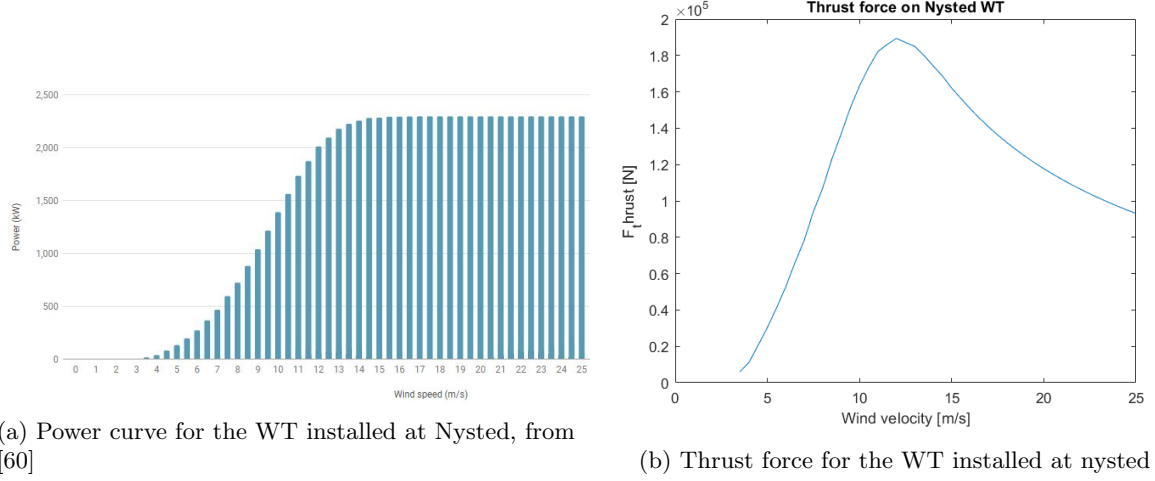


Figure 19

The same procedure can be applied to the WTs installed at Horns Rev I. These WTs are slightly smaller, both in diameter and rated power. The power curve for this WT is shown in Figure 20a[61], and the thrust force graph for Horns Rev I is presented in Figure 20b, with a maximum thrust force of 166 kN.

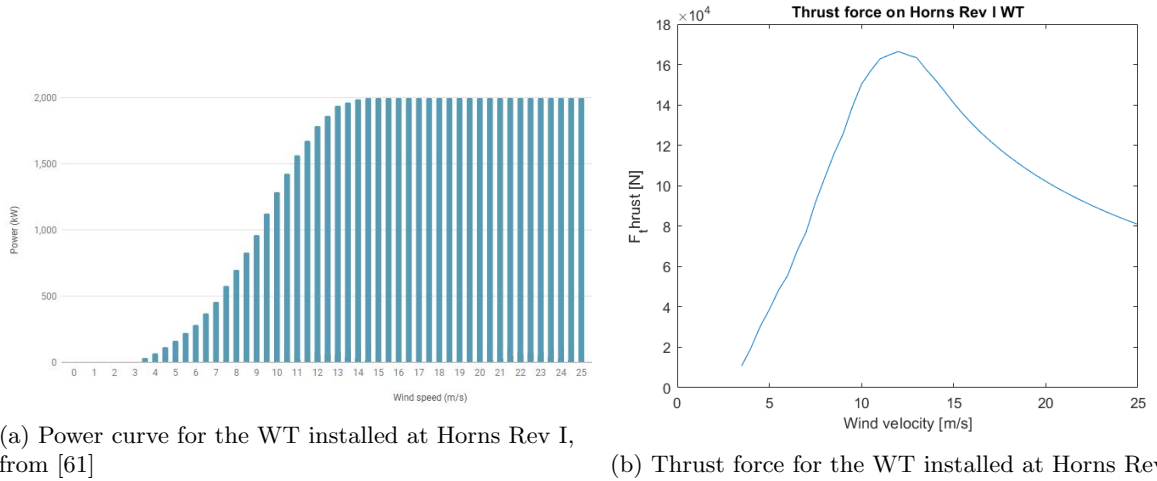


Figure 20

With the horizontal forces due to wind now calculated for both Nysted and Horns Rev I, it is possible to compare them with the AWE system. In Section 3.1.1, the tether force due to wind was already computed. To determine the base shear from this tether force, it must be multiplied by the cosine of the

elevation angle. The graph in Figure 21a shows the horizontal force on the WT and the horizontal part of the tether force in one Figure for the Nysted foundations. In this graph, it can be observed that the force due to the AWE system is more significant in the wind range up until a wind velocity of 9.3m/s, reaching a maximum of 152kN. However, with wind velocities above 9.3m/s, the WT's horizontal force exceeds the AWE system's horizontal force, with a maximum of 189 kN. The graph for Horns Rev I can be seen in Figure 21b. In this case, the AWE system has a more significant base shear until a wind velocity of 9.5m/s, with a maximum of 152kN. For wind velocities greater than 9.5m/s, the WT exhibits a more substantial base shear, with a maximum of 166 kN.

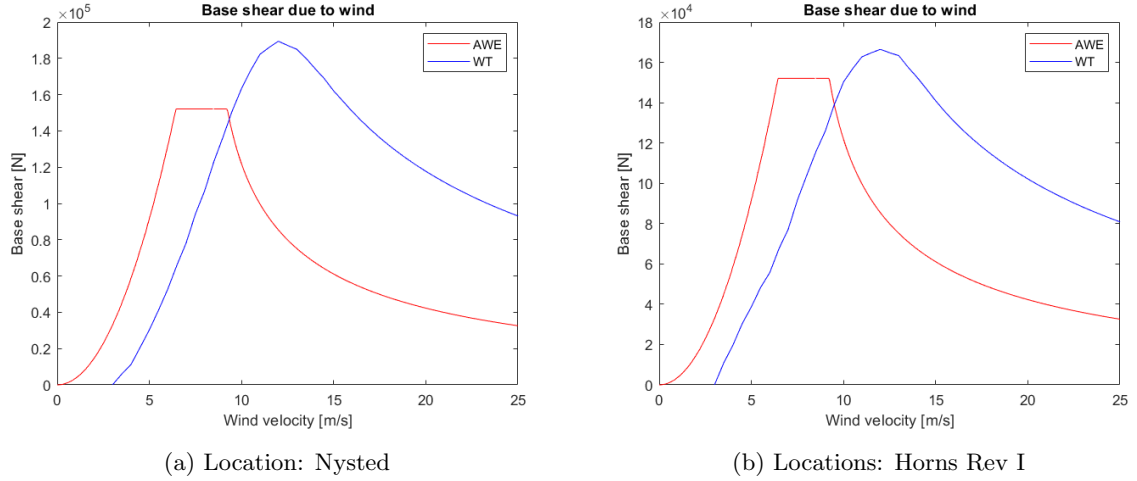


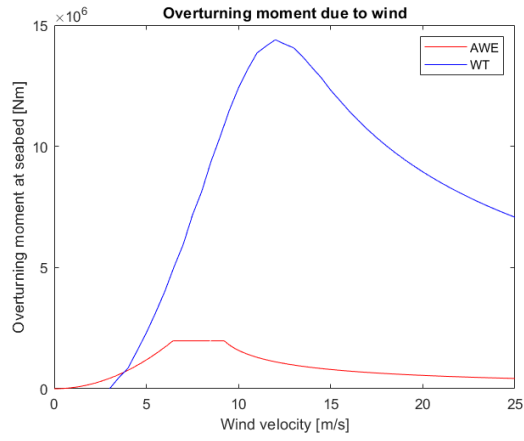
Figure 21: Base shear on foundation caused by wind on AWE system and WT

The consideration of the overturning moment is essential as well. Since the AWE system is a flying kite, a tower is not necessary, allowing the system to be installed directly on the foundation. This significantly reduces the overturning moment. The tower lengths for Nysted and Horns Rev I are 63 m and 70 m, respectively, and the foundation lengths are 13 m and 20 m, respectively. As a result, the AWE system generates a maximum overturning moment of 1.98 MNm for Nysted and 3.04 MNm for Horns Rev I. Comparatively, the original WT at Nysted generates a maximum overturning moment of 14.4 MNm. In contrast, at Horns Rev I, it generates a maximum overturning moment of 15.0 MNm. The graphs are depicted in Figure 22. A summary of the loads is presented in Table 5.

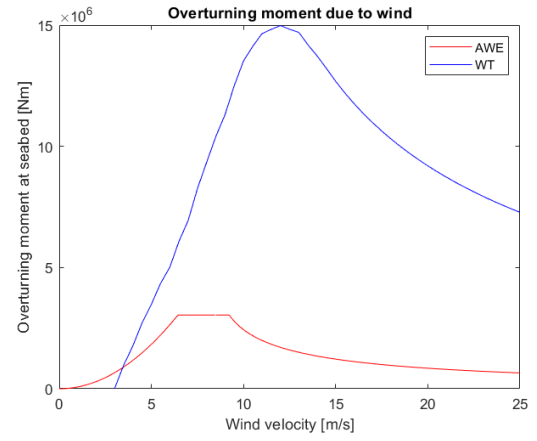
	base shear AWE	Base shear WT	Overturning moment AWE	Overturning moment WT
Nysted	152kN	189kN	1.98MNm	14.4MNm
Horns Rev I	152kN	166kN	3.04MNm	15.0MNm

Table 5: Maximum base shear and overturning moment on foundation due to wind

The analysis confirms that the wind load on the foundations will not exceed the maximum wind loads of the original installations. As a result, the new AWE system will not exceed the ULS for wind loads. Furthermore, since the AWE system does not alter the existing wave loads, the ULS for wave loads will also not be exceeded, as the system is designed to withstand the specified wave loads. It is important to note that while the ULS for wind and wave loads is not exceeded, other aspects, such as fatigue, should



(a) Location: Nysted



(b) Location: Horns Rev I

Figure 22: Overturning moment due to wind by AWE system and WT

still be carefully considered to ensure the foundation's long-term structural integrity and safety when retrofitting with an AWE system.

3.3 Fatigue of foundation

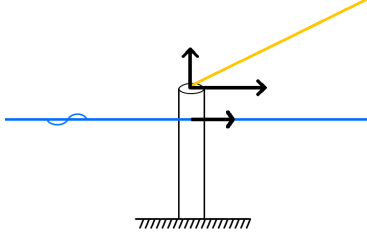


Figure 23: All loads on foundation, simplified

In the preceding sections (3.1.1 and 3.1.2), a comprehensive examination of the loads acting on a foundation revealed their cyclic nature. Subsequently, Section 3.2 determined that the ULS would not be exceeded upon installing a 500kW AWE system. However, given the cyclic loading, analysing potential fatigue-induced damage is imperative.

To assess the fatigue-induced damage on the foundation resulting from cyclic loads, it is essential first to identify all the loads and their corresponding stresses. The foundation is represented as a vertical cylinder fixed to the seabed to simplify the analysis. The cyclic loads consist of horizontal loads at sea level due to waves and the tether loads applied atop the foundation. The tether loads are further divided into horizontal and vertical components. Figure 23 provides a graphical depiction of these loads.

The fatigue damage evaluation relies on S-N curves and Miner's rule.

In this study, the S-N curves specified in design standard C203 for monopile foundations are employed [62]. Additionally, the S-N curve from design standard C502 for concrete foundations is utilised [63]. Specifically, the S-N curve for monopiles is expressed as:

$$\log_{10}(N) = \log_{10}(\bar{a}) - m \log_{10} \left(\Delta \sigma \left(\frac{t}{t_{ref}} \right)^k \right) \quad (33)$$

Here, N represents the number of cycles at stress range $\Delta \sigma$ until failure. $\log(\bar{a})$ corresponds to the intercept of the $\log(N)$ axis, and m denotes the negative inverse slope of the S-N curve. The wall thickness is indicated by t , and the reference thickness t_{ref} is given by t_{ref} , which is 25mm for welded joints. Furthermore, k represents the thickness exponent on fatigue strength. The variables are given in design standard C203 and depend on the corrosion protection and the shape of the structure, as well as the finish of the welds. According to DNV-RP-0416 [64] and DEME's experience, corrosion protection generally lasts 15 years on offshore foundations. Therefore, the S-N curves for free corrosion are applied. The variables for these S-N curves are provided in Table 35 in Appendix A. The structure must be analysed to choose the correct S-N curve from this table. A monopile is a hollow cylindrical shape with circumferential welds. It assumed that these welds were not all dressed flush. This conservative approach is adopted due to the unknown weld finish. Appendix A shows the shapes in Figure 36. The S-N curve matching this shape is identified as curve D. Consequently, the equation for N is derived, incorporating only the structure's wall thickness and stress range as variables:

$$N = 10^{11.687 - 3.0 \log_{10} \left(\Delta \sigma \left(\frac{t}{25} \right)^{0.20} \right)} \quad (34)$$

The fatigue damage for the GBFs is calculated using a different curve specified in design standard C502 [63] for concrete structures:

$$\log_{10}(N) = C_1 \frac{1 - \frac{\sigma_{max}}{f_{rd}}}{1 - \frac{\sigma_{min}}{f_{rd}}} \quad (35)$$

In this equation, C_1 is a constant that can be taken as 8.0 or 10.0, dependent on whether the stress variation is in the compression-tension or compression-compression range. The value for σ_{min} is considered 0 if C_1 is taken as 8.0. The value for f_{rd} can be taken as equal to f_{cd} , which can be calculated by

$$f_{cd} = \frac{f_{cn}}{\gamma_c} \quad (36)$$

The value for f_{cn} is tabulated in DNV C502 [63] and depends on the grade of concrete that is used. For fatigue analysis, the value for γ_c is 1.10.

With the S-N curves for both types of structures now known, the stress ranges should be calculated for the three case studies. The stress acting on the foundations consists of bending stress due to the overturning moment, shear stress due to the horizontal forces, and normal stress due to the vertical component of the tether force. The maximum stresses are used for all stresses, which means that the calculations are done at the seabed. These stresses are calculated separately for different loading scenarios, resulting in eight distinct calculations for the stress ranges. The scenarios include bending, shear, and normal stress ranges during reel-out, bending, shear, and normal stress ranges due to the difference between reel-in and reel-out, and bending and shear stress ranges due to wave loads.

The bending stress is determined using the following equation:

$$\sigma_{bending} = \frac{My}{I} \quad (37)$$

Here, M is the maximum moment: the force for which the stress is calculated multiplied by the height at which this force is acting. The value for y is equal to the radius of the foundation to obtain the maximum stress, and I is the area moment of inertia. The shear stress is calculated with:

$$\tau_{shear} = \frac{V}{A} \quad (38)$$

Here, V is the shear force, and A is the area of the intersection of the foundation. The normal stress is determined with the equation:

$$\sigma_{normal} = \frac{N}{A} \quad (39)$$

Here, N is the normal force, which in this case is the vertical component of the tether force and A is the area of the intersection of the foundation.

The stress ranges can be calculated using these equations by finding the minimum and maximum stress values. The stress range is then obtained by subtracting the minimum stress from the maximum stress. This analysis allows for a comprehensive understanding of how cyclic loading affects the foundation and helps estimate the potential damage caused by fatigue over time.

Based on the provided data, the stress ranges for different loading scenarios on the three foundations are presented in Table 6. Notably, all the stress ranges are low, primarily due to the relatively low overturning moment generated by the AWE system. The wave loads, which remain unchanged, do not cause a significant stress range attributed to the low wave heights and wave periods at both locations. This result is expected since these foundations were designed for a 100-year wave. A 100-year wave results in significantly larger forces and, thus, larger stress ranges. The wave height for which the stress is calculated is the most common at the locations.

The bending stress range due to waves is relatively higher than Nysted and Horns Rev I for the reference OWF. However, this is balanced by a larger load range resulting from higher wave heights and longer wave periods at the reference OWF location.

Overall, the stress ranges calculated indicate that the cyclic loading experienced by the foundations, even with the installation of the AWE system, remains within acceptable limits. The relatively low stress ranges imply that the fatigue damage on the structures is not a significant concern and supports the

conclusion from the ULS analysis that the foundations can withstand the new AWE system without exceeding their design limits.

	Bending reel-out [MPa]	Shear reel-out [MPa]	Normal reel-out [MPa]	Bending reel- in/out [MPa]	Shear reel- in/out [MPa]	Normal reel- in/out [MPa]	Bending waves [MPa]	Shear waves [MPa]
Nysted	0.1018	0.0132	0.0076	0.3043	0.0393	0.0227	0.0981	0.0254
Horns Rev I	0.4508	0.0450	0.0260	1.348	0.1346	0.0777	0.6298	0.1336
reference OWF	0.5219	0.0496	0.0286	1.560	0.1484	0.0857	0.9120	0.1768

Table 6: stress ranges for the different stresses on the three foundations, at seabed

3.4 Expected lifetime

Now that the stress ranges and their corresponding periods for each location are known, the number of cycles until failure and the time it takes to reach this point can be calculated. The result would be eight values for N and eight times until failure. This is impractical and dismisses the fatigue damage inflicted on the foundations. To achieve one value for the lifetime left on the foundation, Miner's rule is employed:

$$\frac{\sum n_i}{\sum N_i} = D \quad (40)$$

In this equation, n represents the number of cycles of a certain stress range that have happened, N is the maximum number of cycles in that stress range until failure, and D denotes the cumulative damage on the structure. If $D = 1$, it indicates that the structure will fail due to fatigue damage. To assess the remaining lifetime of the structure, the yearly damage caused by each stress type is calculated and summed up.

The yearly damage is computed by determining the number of stress cycles of a stress range in a year and dividing that by the maximum number of stress cycles for that particular stress range. This approach takes into account the varying periods of the cyclic loads. By adding up the yearly damage for all eight stress ranges, we obtain a single value for the overall yearly damage.

If the structure is new, the lifetime that is left in the structure could be found by dividing one by the yearly damage. The foundations, however, already have fatigue damage. Accurate fatigue assessment can be achieved through a combination of data-driven and analytical methods[41]. Such an approach involves calculating fatigue using data collected over the years the structures have been operating. This provides a more precise model of the fatigue in the structure since it is based on real-world data rather than predictions. Unfortunately, the data required to perform such a comprehensive fatigue assessment for offshore structures is not publicly available. Therefore, a value for the damage is assumed for this report. The initially assumed value for damage is 80%, meaning there is 20% structural reserve left in the foundations. To calculate the lifetime left in used foundations, the structural reserve must be divided by the yearly damage instead of 1 divided by the yearly damage:

$$YearsLeft = \frac{StructuralReserve}{YearlyDamage} \quad (41)$$

According to design standard DNV-GL-0126 [65], it is imperative to consider design fatigue factor (DFF). For structures without frequent inspection, this factor is 3, which is also used here. This results in a reduced expected lifetime, calculated by the following equation:

$$YearsLeft = \frac{StructuralReserve}{DFF * YearlyDamage} \quad (42)$$

The resulting expected lifetimes for all the foundations, with a 500kW AWE system in the sea state that they are in, are presented in Table 7. For the Nysted foundation, an "infinity" value is shown. The equations for Nysted yield specific numerical values, but for each stress type, the calculated N value significantly exceeds $2 \cdot 10^8$. According to DNV C502 [63], infinite fatigue lifetime may be assumed for concrete structures if the value for N exceeds $2 \cdot 10^8$. At Horns Rev I, the expected lifetime is very long, even with 99% damage to the structure. In this case, the fatigue life could be considered infinite due to the low stress levels resulting from the wave loads. For the reference OWF, the expected lifetimes are noticeably lower, primarily due to the larger waves and longer wave periods at that location. However, the lifetimes are still very long. Even with the 99% damage, the foundation would be structurally viable for retrofitting with AWE. Additionally, the foundation at the reference OWF is slightly longer than at Horns Rev, resulting in larger stress ranges. It is important to note that this reference OWF scenario does not represent an optimal situation, given the considerable water depth, significant waves, and extended wave periods.

	80% damage	90% damage	99% damage
Nysted	∞	∞	∞
Horns Rev I	5091 yr	2545 yr	255 yr
reference OWF	2740 yr	1370 yr	137 yr

Table 7: Expected lifetimes of foundations retrofitted with AWE for different levels of initial fatigue damage on the foundations

Overall, the results indicate that installing a 500kW rated power AWE system would generally not cause the foundations to reach their fatigue limit within a reasonable time frame. The lifetimes of all the foundations remain substantial and exhibit extended fatigue life.

4 Optimization

In Section 3.3, it was determined that the foundations have a very long fatigue life remaining if retrofitted with AWE. This raises the question of whether the system can be optimized to utilize more of the structure's potential. In this section, two possibilities for optimization are considered. Firstly, the option of leaving the existing tower and placing the AWE system on top of it is explored, where the AWE system would replace the rotor nacelle assembly (RNA). Secondly, the potential of using a larger AWE system is considered, although this may not be very realistic in the short term.

4.1 Replacing RNA with AWE system

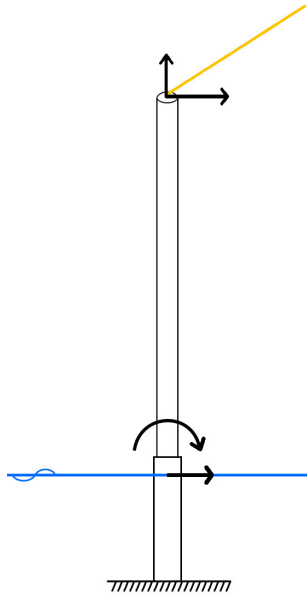


Figure 24: All loads on foundation and tower, simplified

Leaving the OWF towers in place could be a more economical option, as it would require even less removal of the OWF. Further details on the economic aspects are elaborated in Section 5. Moreover, placing the AWE system on top of the tower enables the kite to fly at higher altitudes with the same elevation angle or at the same height with a lower elevation angle. Higher altitudes would offer more consistent and higher wind velocities, resulting in improved electricity output. Lower elevation angles allow the system to work more efficiently, as the kites can fly in a more true crosswind pattern, maximizing the usable wind velocity. Therefore, placing the AWE system atop the tower is expected to enhance electricity production. The tether forces and power output are recalculated to assess this possibility, considering a lower elevation angle. Subsequently, the new tether forces are used to recalculate the base shear and overturning moment. Since the tower length contributes to the overturning moment, its effect is accounted for. The stresses, including those in the tower, are recalculated based on the new base shear and overturning moment. The loads are depicted in Figure 24. The moment at the top of the foundation accounts for the effect of the long tower on the foundation, resulting in bending stresses due to wind in both the tower and the foundation. Table 8 provides a summary of the dimensions of the towers, which are used in the stress and lifetime calculations for the scenario with the AWE system placed on top of the tower.

	Tower length	tower diameter	Tower wall thickness
Nysted	63m	3.5m	$D/t = 120$
Horns Rev I	70m	3.6m	$D/t = 120$
Reference OWF	70m	3.0m	$D/t = 120$

Table 8: Tower dimensions

Table 9 presents the results of the calculations. For Nysted, all the values for N for the foundation are still larger than $2 \cdot 10^8$, indicating an infinite fatigue life. However, the tower is made out of steel, not concrete. Therefore, the lifetimes in the table for Nysted are the fatigue lifetimes of the tower. For Horns Rev I, the lifetime is significantly reduced compared to placing the AWE system on top of the foundation. Due to the DFF, a damage percentage of a maximum of 42% is allowed to ensure a lifetime of 25 years. This might still be realistic, depending on the weather at that OWF in the past 20 years. On the reference OWF, an AWE system cannot be placed on top of the tower. The increased stresses,

combined with the DFF of 3, make the lifetimes too short to consider this. It should be noted that this is not a real OWF but a mere example of the possibilities.

	43% damage	77% damage	80% damage	90% damage
Nysted	61 yr	25 yr	22 yr	11 yr
Horns Rev I	25 yr	10 yr	8.8 yr	4.4 yr
Reference OWF	5.2 yr	2.1 yr	1.8 yr	0.9 yr

Table 9: Expected lifetimes of foundations retrofitted with AWE on top of tower

4.2 Larger AWE system

Based on the information provided in Sections 3 and 4.1, it can be inferred that the 500kW AWE system may not be optimally sized for the existing offshore foundations. However, the selection of the 500kW system is justified, as explained in Section 2.1. Nonetheless, exploring the potential of larger AWE systems that the foundations can withstand is of interest. In this section, the size of the AWE system is increased to 2MW, which is close to or equal to the original rated power values. The characteristics of the 2MW AWE system are based on data from [27] and the Ampyx AP4 2MW kite model [36]. The key characteristics of the increased AWE system are tabulated and compared to those of the 500kW system in Table 10.

	Wing area	Flight height	Lift/drag ratio	Tether diameter
500kW	45 m^2	200m	15	0.02m
2MW	109 m^2	500m	15	0.05m

Table 10: AWE characteristics, modified from [27]

With a larger power output, the tether force increases significantly. If the tether diameter is limited to 0.05m, the maximum tether force is 703kN for the 2MW AWE system, compared to 152kN for the limited 500kW system. This immediately raises concerns about the base shear of the foundation. As discussed in Section 3.2, the base shear caused by the wind in the wind turbines was calculated to be 166kN and 189kN. A maximum tether force of 703kN results in a base shear of 608kN. To address this issue, the calculations for the ULS must be revisited to verify whether the foundations can withstand the increased base shear. Alternatively, limiting the tether force to maintain the maximum base shear at its original value of 166kN or 189kN is possible, but this would significantly reduce the power output, which is undesirable.

The fatigue calculations can proceed, assuming that the maximum tether force of 703kN is acceptable. Taking 80% and 90% to the structure, the expected fatigue lifetimes for the foundations are shown in Table 11. The damage percentage of 25 years of lifetime left for the different locations is also shown in Table 11.

	80% damage	90% damage	96% damage	97.4% damage
Nysted	∞	∞	∞	∞
Horns Rev I	190 yr	95 yr	38 yr	25 yr
Reference OWF	125 yr	63 yr	25 yr	16 yr

Table 11: Expected lifetimes with 2MW AWE system installed

The results in Table 11 indicate that, depending on the initial amount of fatigue damage on the foundations, fatigue may not be the determining factor. Even with 96% damage for the reference OWF and 97.4% damage for Horns Rev I OWF, the expected fatigue lifetime remains at 25 years.

With the increased base shear for the 2MW AWE system, the ULS must be validated. For Horns Rev I, this is done with ISO19902 [66]. The foundation is subjected to a shear load from wind and waves, a bending moment due to wind and waves and an axial tension due to wind loads. The conditions for shear load, bending loads, and axial tension for ULS are given by Equations 43, 44, and 45, respectively. The values are compared in Table 12, where E is assumed to be 210 GPa and the representative yield strength f_y is 300 MPa, typical values for steel.

$$\tau_b = \frac{2V}{A} \leq \frac{f_v}{\gamma_{R,v}} \quad (43)$$

$$\sigma_b = \frac{M}{Z_e} \leq \frac{f_b}{\gamma_{R,b}} \quad (44)$$

$$\sigma_t = \frac{F}{A} \leq \frac{f_t}{\gamma_{R,t}} \quad (45)$$

	$\frac{2V}{A}$	$\frac{f_v}{\gamma_{R,v}}$	$\frac{M}{Z_e}$	$\frac{f_b}{\gamma_{R,b}}$	$\frac{F}{A}$	$\frac{f_t}{\gamma_{R,t}}$
Horns Rev I	1.21 MPa	165 MPa	1.96 MPa	367 MPa	0.307 MPa	285 MPa
Reference OWF	1.37 MPa	165 MPa	2.49 MPa	367 MPa	0.402 MPa	285 MPa

Table 12: ULS values next to the calculated values with a 2MW AWE system

Table 12 clearly shows that the ULS is not nearly reached for each stress type. This is because the wave forces are calculated based on the wind velocity at which the tether forces peak. If the wave forces are calculated for ULS, the stresses due to these wave forces are more significant. However, during such peak events, the kites are either not flying or experience significantly lower forces than the peak value of 703kN. This, combined with the reduced overturning moment, ensures that the 2MW AWE system is still suitable for the foundations at ULS. This also shows that these foundations are designed with ULS in mind and not FLS. The foundations can withstand 100-year waves; therefore, the increased tether force at specific wind velocities will not affect the ULS of the system.

4.3 Larger AWE system replaces RNA

With the calculations done for a small AWE system on top of the tower and a larger AWE system on the foundation, only the possibility of a larger AWE system on top of the tower remains an option for optimization. Considering the values from Table 9, this is not a realistic option. The calculation results are shown in Table 13. The expected lifetimes are very low due to the large overturning moment and horizontal force. The towers and foundations are not designed for this kind of load on top of the tower, and therefore, it is structurally not viable to replace the RNAs with 2MW AWE systems.

	0% damage
Nysted	0.09 yr
Horns Rev I	0.69 yr
Reference OWF	0.14 yr

Table 13: Expected lifetimes with 2MW AWE system installed on top of tower

5 Economics

Retrofitting offshore wind foundations with AWE systems holds promise in terms of structural advantages, but the success of such a project is contingent upon its economic viability. The income and costs must be assessed comprehensively to determine the economic feasibility. This section considers four distinct scenarios to evaluate the economic viability of AWE retrofitting for OWFs.

In the first scenario, the OWF is retrofitted with 500kW AWE systems mounted on the existing foundations. In the second scenario, the towers are retained, and the AWE system is installed on top of the tower to replace the traditional RNA. A third scenario involves repowering the OWF, wherein the entire old OWF is dismantled, and a new OWF with larger WT's is constructed at the same location. This scenario is added to provide a comparison with a competitive alternative. Lastly, there is the scenario of decommissioning the OWF and not replacing it with anything. All of these scenarios are applied to both of the previously discussed potential OWFs: Nysted and Horns Rev I.

To conduct a fair comparison among the scenarios, the income generated by each option is calculated. Subsequently, the associated costs are carefully analyzed. With this information, the NPV and LCoE can be calculated and employed to compare the different scenarios, enabling an informed assessment of their economic viability.

5.1 Income

An OWF's income depends on its electricity production, which, in turn, is highly influenced by the prevailing wind velocity and its consistency throughout the year. A higher-rated power for WT's may imply greater electricity generation potential. It is, however, crucial to account for the wind velocities at the specific location. Figure 25a depicts the power curves for three different systems: a 500kW AWE system, a 2.3MW WT (representing the original WT at Nysted), and a 10MW WT [67]. The power curve for the AWE system mounted on top of the tower is omitted as it closely resembles the 500kW AWE power curve when mounted on the foundation. The graph illustrates that the maximum power output for the WT's is achieved at approximately 14m/s wind velocity. However, this is not the most common wind velocity at the study locations. The most common wind velocity for both Nysted and Horns Rev I falls within the range of 5.3m/s to 7.8m/s [68], resulting in non-ideal conditions and relatively low capacity factors for both WT's. The graph also shows that, although not ideal, the 10MW WT is more effective at this location than the original 2.3MW WT. Figure 25b further demonstrates the hours of wind velocities in a year on the right axis of the graph. With the two figures combined, it can be seen that the prevailing wind velocities do not accommodate the WT's.

The annual electricity production for all systems can be estimated and compared using the power curves and the hours of wind velocities at the respective locations, the annual electricity production for all systems can be estimated and compared. This is done by multiplying the annual hours for specific wind velocities by the respective system's power output at each wind velocity. Adding up all the wind veloci-

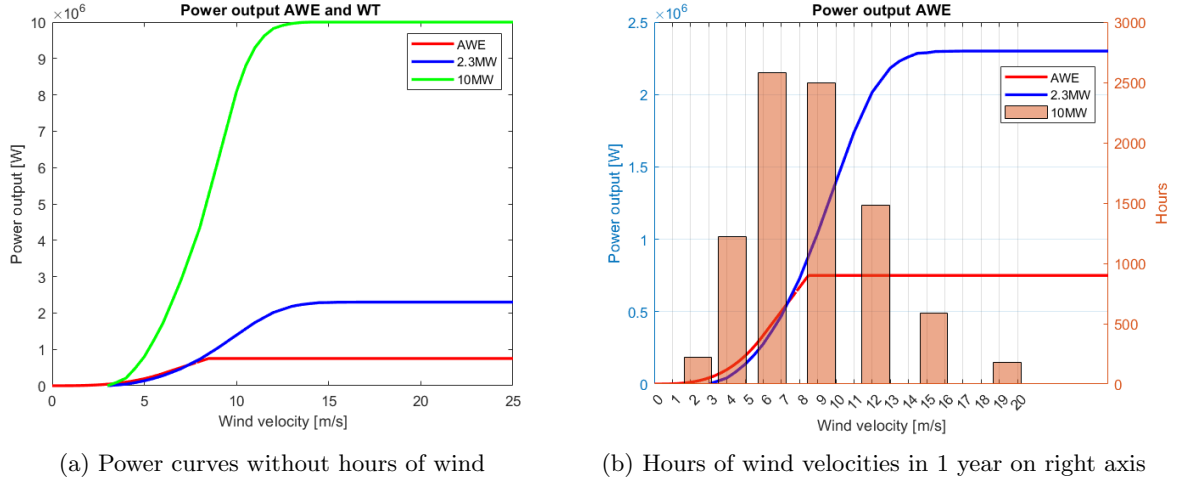


Figure 25: Power curves of 500kW AWE system, 2.3MW WT and 10MW WT

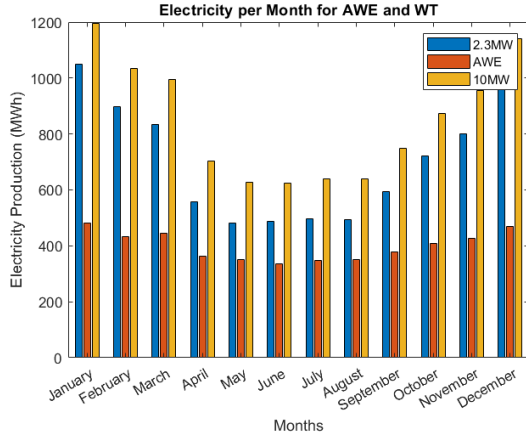
ties results in the annual electricity production for each system, and monthly energy production graphs can be plotted. Table 14 presents the calculated values for yearly electricity production and capacity factors per AWE system or WT. Figure 26 illustrates the monthly electricity production comparisons for the three systems at Nysted and Horns Rev I. In this table and these figures, the values for electricity production of the 10MW WT are corrected for the number of WTs possible at the locations. Both sites can accommodate a maximum of 16 10MW WTs, as explained later in this section. It is important to note that the table and the figure values are for single systems and not in a wind farm configuration.

The findings show that the 10MW WTs work more efficiently in the current conditions at the locations, leading to higher capacity factors than the original WTs. Nevertheless, there is a notable variation in the seasons for the WTs due to the higher wind velocities in winter and relatively lower wind velocities in summer. In contrast, the AWE system maintains a more consistent electricity production throughout the year, resulting in a higher capacity factor.

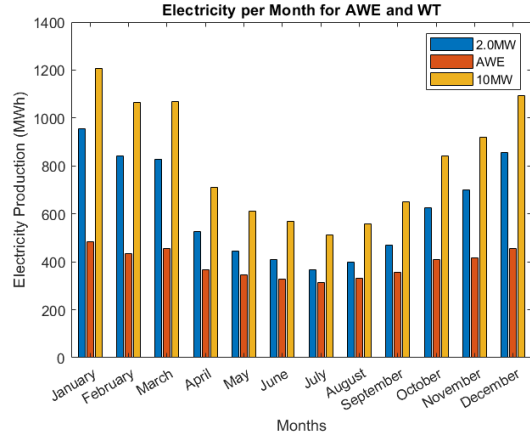
	AWE	c_p	Original WT	c_p	10MW WT	c_p	AWE on tower	c_p
Nysted	3191 MWh/yr	0.73	8409 MWh/yr	0.48	10176 MWh/yr	0.51	3361 MWh/yr	0.77
Horns Rev I	3123 MWh/yr	0.71	7421 MWh/yr	0.42	9816 MWh/yr	0.49	3313 MWh/yr	0.76

Table 14: Yearly electricity production and capacity factors per AWE system or WT

To calculate the yearly electricity production of an OWF, it is imperative to consider the wake effects caused by the WTs and, potentially, the AWE systems. To account for wake effects in a wind farm setting, it is crucial to consider the layout of the OWF. Wake effects can greatly decrease the capacity factors for both WTs and, potentially, AWE systems. This study calculates wake effects for the scenario where the OWF is repowered with 10MW WTs. Proposed layouts for Nysted and Horns Rev I, considering the spacing between WTs and the prevailing wind direction, are depicted in Figure 27. The proposed layout



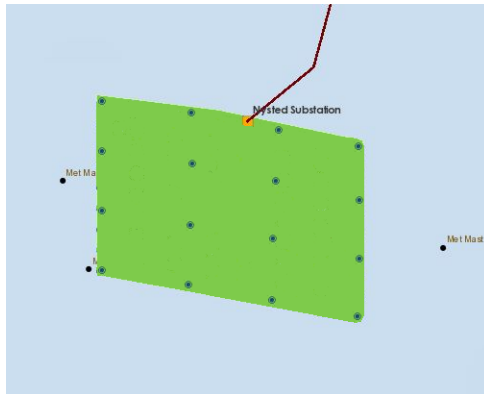
(a) Nysted



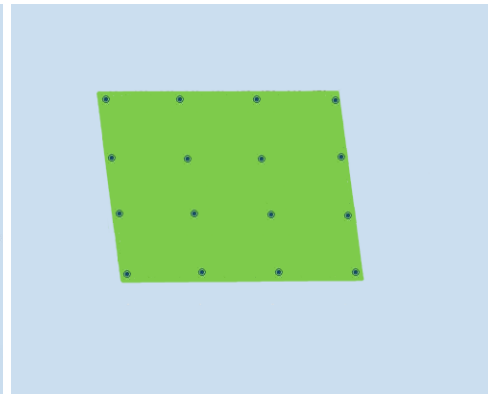
(b) Horns Rev I

Figure 26: Monthly electricity production comparisons for three systems at two locations

assumes a spacing of 10D in the dominant wind direction. In other directions, the spacing is 7D, where D represents the turbine diameter of 193 meters[67].



(a) Nysted



(b) Horns Rev I

Figure 27: Proposed layout for OWF with 10MW WTs. Spacing in wind direction: 10D

The wake effect is calculated using an Excel tool based on the Jensen wake model. The overall row efficiency is calculated to be 59% for the most common wind velocities, with the efficiency increasing at higher wind velocities. This number is deficient for this OWF, with the number of WTs in a row and spacing between the WTs. However, a more accurate calculation does not fall within the scope of this study. Section 5.3 provides further details on this. The row efficiency is calculated based on the most common wind velocity throughout the year for both locations. For Nysted, with four rows of four turbines, a yearly electricity production of 44.2 GWh per 10MW WT and a row efficiency of 59%, the result is a total electricity production of 417GWh per year. For Horns Rev I, with slightly different wind conditions, the calculated electricity production is 402GWh per year. The wake effects of rigid AWE systems in OWFs are still unknown; however, the losses due to wake effects are expected to be

limited compared to WTs. This is primarily because AWE systems employ a single wing instead of the three-blade configuration of traditional WTs, resulting in less air disturbance, which is spread over a much larger vertical spacing due to the flight pattern of the kite [69]. Furthermore, AWE systems can be optimized to fly at different heights, reducing wake effects. Simulations have been done for wake effects in AWE wind farm layouts. The wake losses were found to be between 8.5% and 18% in wind farm layouts with a spacing of $2/L^2$ [70]. Using the original layouts, the spacing for an AWE OWF would result in a spacing of $0.25/L^2$. This is four times more area per AWE system. Therefore, the wake effects are even further reduced. Consequently, the row efficiency for the AWE systems in the proposed layout is assumed to be 95%.

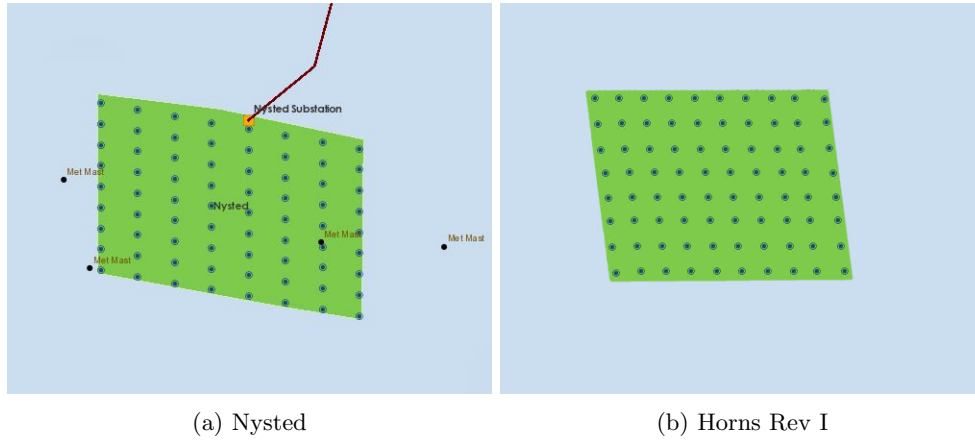


Figure 28: Original layouts for the Nysted and Horns Rev I OWFs

When mounted directly on the foundation or on top of the tower, the AWE systems would be integrated into the original layouts, differing only in the height of the AWE systems. Figure 28 displays the layouts for Nysted and Horns Rev I. Nysted comprises nine rows of foundations with eight foundations each, while Horns Rev I consists of eight rows of ten foundations. The yearly electricity production for a 500kW AWE system at Nysted is estimated at 3192 MWh. Considering eight foundations in a row and an assumed row efficiency of 95% per row, this results in 27.3 GWh per row. With nine rows, the estimated annual electricity production at Nysted is 218 GWh. A similar calculation for Horns Rev I yields an annual electricity production of 237 GWh, slightly higher than at Nysted. The main reason for this difference is the higher number of foundations at Horns Rev I, which allows for more AWE systems to be installed. The capacity factors for both locations are similar, with 0.69 for Nysted and 0.68 for Horns Rev I when mounted on top of the foundations. When mounted on the tower, the capacity factors are higher, yet similar for both locations. All the results are summarized in Table 15.

	AWE	c_p	10MW WT	c_p	AWE on tower	c_p
Nysted	218 GWh/yr	0.69	417 GWh/yr	0.30	230 GWh/yr	0.73
Horns Rev I	237 GWh/yr	0.68	402 GWh/yr	0.29	252 GWh/yr	0.72

Table 15: Summary of yearly electricity production and capacity factor per system and location in OWF setting

Table 15 shows that the income generated by a 10MW WT is significantly higher. However, this higher

income comes at the cost of removing the existing foundations and building an entirely new OWF. This higher income is a result of the larger initial investment. The income generated by the AWE system mounted on the tower is also higher due to the lower elevation angle, resulting in greater electricity production efficiency. The cost of all systems and at all locations are calculated in subsequent calculations. Then, the least expensive system will be determined.

5.2 Costs

The costs of each scenario are at least equally important as the income. From Section 5.1, it was established that the OWF with 16 10MW WT would generate the most revenue, followed by AWE systems at Horns Rev I and AWE systems at Nysted. In this section, the cost will be broken down for each separate system, including the cost of decommissioning, commissioning and maintenance of each system. Order of operations and practicalities are considered as well. This is done to ensure a cost figure that is as realistic as possible.

5.2.1 AWE on foundation

To calculate the costs of retrofitting the foundations with a 500kW rigid wing AWE system, it is imperative to know the costs of these systems. These systems, however, do not exist yet. Therefore, an estimate is done for the full costs of the system. The estimate is based on values from the literature. After the costs of the system are known, an estimation can be made for the cost of removal of the RNA and the tower and the installation of the AWE system.

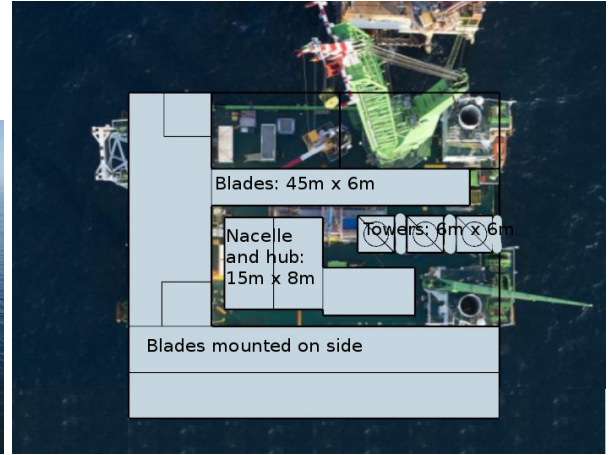
The cost of a rigid kite AWE system is estimated between €2820000/MW and €3700000/MW [70]. These values are based on other literature and ongoing research. The foundations in shallow water are included in these costs. In [55], the costs of rigid wing AWE systems are estimated to be €1900000/MW. This excludes foundations; therefore, this number is also used in this study. This results in a rigid wing 500kW AWE system costing €950000.

It is assumed that the ground stations of the AWE systems are built specially for this project. By doing that, the ground station can be modified to be bolted on the foundation without any modifications. The RNAs and towers must be removed first for this to happen. This is done with a jack-up vessel. An example of such a vessel would be Neptune from DEME, shown in Figure 29a. Such an operation would consist of positioning the vessel, jacking up, removing the blades one by one, removing the nacelle and hub, and removing the tower. After this, the vessel can go down again and sail to the next location. As shown in Figure 29, all the components will be placed on the jack-up vessel. This shows that there is deck space for nine blades on the vessel if the vessel is extended sideways. Looking from above in Figure 29b, an arrangement on the vessel can be made so that three towers and three nacelle/hub assemblies can fit on the vessel for transportation.

According to [31], the time for turbine installation from the moment of positioning the vessel to the moment the vessel leaves the site is approximately 24 hours. This takes so long during installation because the components must not be damaged. When removing the components, this is of less importance. Therefore, the time for removal can be assumed to be shorter. In this case, the time it takes from positioning to leaving the site is assumed to be 18 hours. After leaving the first site, the vessel will sail 800 meters to the next site and start over. The sailing time between foundations is 15 minutes, assuming a 10 knots or 5m/s velocity and time needed to accelerate and decelerate. After removing three WTs, the vessel must sail back to shore to unload. The distance to the nearest harbour for Nysted is 25km, and for



(a) Jack-up vessel Neptune in operation, image from [71]



(b) Jack-up vessel Neptune from above with possible arrangement, image from [71]

Figure 29: Jack-up vessel Neptune, images from [71]

Horns Rev I, it is 35km. This results in a cycle time of 65 hours for three WT removals. This includes 2 hours of sailing to and from the OWF and 7 hours of unloading at the harbour. This results in 65 days to remove the WTs at Nysted and 73 days to remove the WTs at Horns Rev I, assuming that weather conditions allow for continuous operation. From [31], a day rate for the vessel of €200000 is used. This is adjusted for ship size, inflation and currency conversion. Therefore, while keeping the foundations in place, the total cost of WT removal is €13 mln for Nysted and €14.6 mln for Horns Rev I, assuming weather conditions allow for WTs removal. The results are summarised in Table 16.

	No. of WTs	Duration	Total cost	Cost per WT
Nysted	72	65 days	€13 mln	€180556
Horns Rev I	80	73 days	€14.6 mln	€182500

Table 16: Duration and cost of WT removal for Nysted and Horns Rev I OWFS

It is recommended to perform the extraction of WTs and installation of the AWE system simultaneously to save time. This approach eliminates the need for frequent repositioning and jacking up of the vessel, thereby improving efficiency. The deck space can accommodate the three additional AWE systems because the AWE systems are unloaded when the WTs and towers are loaded onto the vessel. It should be noted that the installation of AWE systems will require a significant amount of additional time. Specifically, approximately three hours will be needed to rewire and prepare the foundation and lift, bolt, and connect the AWE system. This means the overall time required to remove WT and install AWE will be 21 hours from when the vessel is positioned until it departs the site. Consequently, the cycle time for three foundations will be extended to 74 hours, which increases the project's duration and cost. However, installing AWE systems immediately upon removing the WT is worthwhile, as it shortens the overall project duration. The costs are summarised in Table 17. Maintenance costs should be considered as well. This is similar for both AWE systems and is discussed in detail in Section 5.2.3.

	No. of WTs	Duration	Total cost	Cost per WT
Nysted	72	74 days	€14.8 mln	€205556
Horns Rev I	80	83 days	€16.6 mln	€207500

Table 17: Duration and cost of WT removal and AWE installation for Nysted and Horns Rev I OWFs

5.2.2 AWE on tower

In Section 4.1, it was concluded that it is structurally possible to leave the tower in place and replace the RNA with the AWE system. This results in a slightly more efficient system due to the lower elevation angle. It could also possibly lower the cost of the WT removal since the towers do not have to be removed. However, installing the AWE system on top of the tower is more challenging and costs more than installing an AWE system on the foundation. In Section 5.2.1, it was established that removing blades, nacelle and hub, and tower takes 18 hours. It is assumed that removing the tower will take three hours, according to the timeline in Table 18.

Positioning and jack up	4 hours
Blade removal 3 blades	6 hours
Nacelle + hub removal	3 hours
Tower removal	3 hours
Jack down + leaving site	2 hours

Table 18: Timeline WT removal

In Section 5.2.1, it was assumed that installing the AWE system on the foundation would add 3 hours to the operation. In this case, the complete AWE system must be hoisted to the top of the tower and connected there. This must be done very carefully so as not to damage anything. Therefore, it is assumed that the complete installation of the AWE system on top of the tower will add another 3 hours to the operation. The result is that installing the AWE system on top of the tower will take as long as installation on the foundation. Leaving the tower in place does not leave enough deck space on the vessel to accommodate more WT blades; therefore, the cycle time also does not change. Installing the AWE system on top of the tower will cost the same as installation on the foundation. The costs are summarised in Table 17.

5.2.3 AWE maintenance

The AWE system and foundations must be maintained. The costs for maintenance are unknown since the rigid wing 500kW AWE system does not exist yet. However, for WTs in OWFs, the OPEX is 3% of the complete CAPEX. In [70], it is stated that the OPEX for AWE is lower than for WTs. Values from the industry (Ampyx) also suggest an OPEX of 2.3% for the AWE system. This excludes the OPEX for the foundations. The tether of the AWE system is sensitive to fatigue damage. As a result, the tether must be replaced every five years for €35000 per system. According to [31], the maintenance for the BoP, which includes the foundations and substations, is €4 mln per annum. Operations and logistics add up to €5.6 mln. With a CAPEX of €950000 for the AWE systems, the OPEX results in €21850 per system, resulting in an AWE OPEX of €1.57 mln for Nysted and €1.75 mln for Horns Rev I. Therefore, the system's total OPEX is €11.57 mln per year for Nysted, and €11.35 mln per year for Horns Rev I and €2.5 mln per five years for Nysted for the tether and €2.8 mln per five years for Horns Rev I. The costs are summarised in Table 19.

	AWE OPEX	BoP OPEX	Operations	Total OPEX
Nysted	€1.57 mln	€4 mln	€5.6 mln	€11.17 mln
Horns Rev I	€1.75 mln	€4 mln	€5.6 mln	€11.35 mln

Table 19: OPEX breakdown for AWE system per annum

	No of WTs	Duration	Total cost	Cost per foundation	Total cost WT + foundation
Nysted	72	36 days	€9 mln	€125000	€23.8 mln
Horns Rev I	80	45 days	€9 mln	€112500	€25.6 mln

Table 20: Cost and duration of foundation removal and total cost OWF removal

5.2.4 Repowering with 10MW WT

To upgrade the OWFs with 10MW WTs, removing both the WTs and the foundations is necessary. The increased rated power per WT renders the existing cables unusable, necessitating their removal. However, the substation may still be viable for reuse, as the total rated power of the OWF is not increasing. Once the old OWF has been removed, the installation of the new one involves new foundations, cables, and WTs. To begin this process, the WTs must first be removed, as described in Section 5.2.1, with the associated costs summarized in Table 16. Once the WTs have been extracted, the foundations can be removed. According to [31], this is accomplished by cutting a monopile 1 meter below the seabed. Industry estimates suggest that it will take 12 hours to remove each foundation and that eight monopiles of 20m can fit on a vessel for transportation to shore. As a result, it will take 45 days to remove the 80 monopiles at Horns Rev I for €9 million. For Nysted, the situation is different. The gravity-based foundation can be deballasted and floated off to be broken down. The foundations have a diameter of 15.4m at the lower part, making it difficult and inefficient to load them onto a vessel for transportation. Instead, they can be towed back to the harbour. Deballasting will take 12 hours[31]. Therefore, this continuous cycle will take only 36 days. Assuming the tug boat has a day rate of €50000, this will cost €9 mln. The costs of the foundation, WT, and foundation removal are summarized in Table 20.

When considering the removal of cables, it is essential to evaluate the costs and benefits carefully. According to [31], removing cables can be expensive due to the need to extract them from under the seabed. Until techniques are perfected, it is only logical to remove cables if the conducting material's value is greater than the removal cost. This study assumes that the cost of removing the cables exceeds the value of the materials, and, therefore, they will be left in place. Nonetheless, this decision can be reevaluated towards the EoL of the new OWF, should new techniques emerge that make it more cost-effective to remove the original cables.

After removing old WTs and foundations, the installation of new WTs and foundations can begin. The cost of a new WT, which includes the tower, is typically €10 million per WT. In addition, new array cables and foundations will be required. The average cost of array cables for a 10MW WT is around €350000 per WT. The cable that connects the OWF to the shore and substation can be reused since the rated power of the OWF will not change. However, the substation will require new electrics, costing around €600000 per WT. The cost of the foundations, which include monopile, transition piece, scour protection, and corrosion protection, is €3.78 million per foundation. Overall, the total cost of the components necessary for repowering the OWF with a 10MW WT is €14.73 million per WT or €235.7 million in total. All figures are sourced from [31], adjusted for inflation and exchange rate.

According to the report by BVG associates [31], installing a single monopile has a cycle time of 2 days, with a day rate for the vessel of €270000 per day. The installation of the WT on the foundation takes

24 hours, and the vessel can carry two complete WT's to the site of the OWF, resulting in a cycle time of 2.5 days for two WT's. Cable installation has a cost of €600000 per WT. Consequently, the cost of the foundation installation is €8.64 mln, the cost of WT installation is €5.4 mln, and the cost of cable installation is €9.6 mln, making the total installation costs €49.6 mln. All the costs are summarised in Table 21.

	Removal	New components	Installation	Total
Nysted	€23.8 mln	€235.7	€49.6 mln	€309.1 mln
Horns Rev I	€25.6 mln	€235.7	€49.6 mln	€310.9 mln

Table 21: Total CAPEX of 10MW WT OWF at Nysted and Horns Rev I

An essential factor to consider is the operational costs of an OWF. According to BVG associates[31], these costs are typically 3% of the CAPEX per annum. In this case, that means an OPEX of €9.3 mln per year for both OWFs.

5.2.5 Only decommissioning

The fourth option is to decommission the OWF whenever it is not economically or technically viable to operate the OWF and to not replace it with anything else. If this were the case, the site of the OWF has to be completely cleared. That means that not only the WT's and foundations must be removed, but the substation and cables as well. In Section 5.2.4, it was determined that the removal of the foundations and WT's cost €23.8 mln for Nysted and €25.6 mln for Horns Rev I. The removal of the substation is assumed to be a three-day operation with a vessel at a €200000 day rate. The result is €600000 to remove the substation. After the substation has been removed, the foundation can be removed. This is assumed to be the same cost as the WT foundations at €115000 for Nysted and €112500 for Horns Rev I. The total removal for the substation is, therefore, €715000 for Nysted and €712500 for Horns Rev I. It is assumed that the remaining value of the cables covers the cost of the removal. Therefore, the cost of the cable removal is not further elaborated on.

To make a fair comparison with the other scenarios, the cost of the full decommissioning is adjusted for inflation over 25 years. This inflation is assumed to be 3%. In Section 5.3, this scenario is added to the NPV in tables 22 and 23.

5.3 Results

With the costs and incomes known, the NPV and LCoE can be calculated. For both, a discount rate is necessary. This discount rate is chosen conservatively at 7%. The LCoE shows the cost of energy produced by the OWFs, levelized over the years the OWF has been in operation. It takes the CAPEX, OPEX and DECEX into account. The NPV graph will show if the project is profitable over the years. When NPV is above zero, the project is worthwhile.

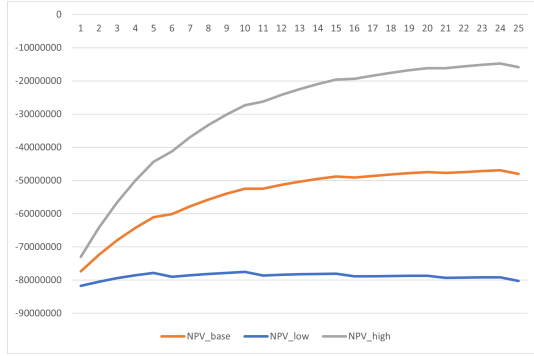
5.3.1 Nysted

The NPV for installing AWE systems on the foundations at Nysted is shown in Figure 30a. In this figure, the NPV is calculated for three possible prices for energy. The low price is €60/MWh, the base price is €80/MWh, and the high price is €100/MWh. It can be seen that the NPV does not reach zero for any of the energy prices. That means the project would not be profitable over 25 years due to the discount rate and inflation. It is, however, important to note that this NPV includes partial decommissioning of the old OWF, something that has to happen anyway. For Nysted, the cost of partial decommissioning is

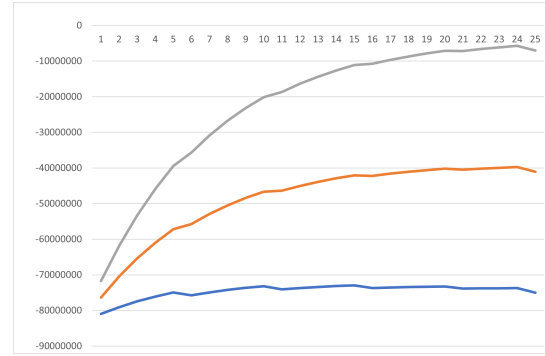
€13 mln. The balance after 25 years at the high price case is -€16 mln. Consequently, the installation of AWE systems covers parts of the cost of decommissioning the original OWF. The LCoE for this scenario is €85.30/MWh.

Alternatively, the complete OWF can be removed, and 16 new 10MW WT can be installed. Due to the higher rated power of this OWF, the revenue is larger. However, the cost is also much larger, resulting in a graph for the NPV as shown in Figure 30c. The low, base and high prices are the same values as in Figure 30a. Due to the larger investments necessary for this project, the NPV for the high price results in -€64 mln. This is mostly due to the low capacity factor for the complete OWF of 0.30. Suppose the OWF efficiency could be increased so that the OWF capacity factor would be 0.36; the NPV for the high price results in a positive number. The LCoE for this scenario is slightly lower than the LCoE for AWE at Nysted, with €82.71/MWh.

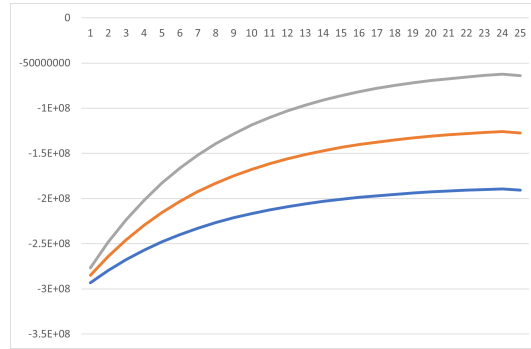
In the last scenario, the AWE systems are mounted in place of the RNA. The result is not a cheaper installation because it is more challenging. The electricity production, however, is higher because the elevation angle is lower. This results in higher revenue and, therefore, a more promising NPV. The NPV for the AWE systems mounted on top of the tower at Nysted is shown in Figure 30b. The decommissioning costs for this system are higher because the tower still has to be removed when the OWF is at the EoL. The higher electricity production results in an NPV of -€7.0 mln. This completely covers the cost of the partial decommissioning of the original OWF. The LCoE for this scenario is €80.74/MWh.



(a) NPV for AWE on foundations at Nysted



(b) NPV for AWE on the tower at Nysted



(c) NPV for 16 10MW WTs at Nysted

Figure 30: NPVs for Nysted. Low price: €60/MWh, base price: €80/MWh, high price: €100/MWh

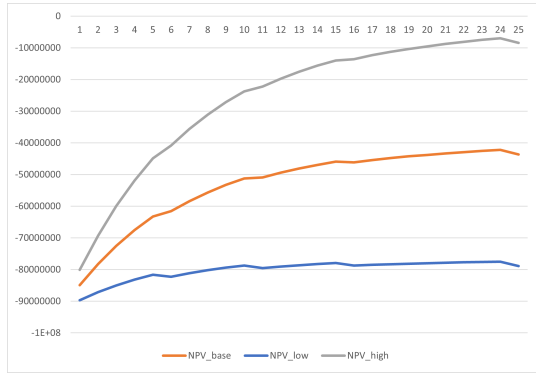
Scenario	NPV after 25 years	LCoE
AWE on foundation	€-16 mln	€85.30/MWh
AWE on tower	€-7.0 mln	€80.74/MWh
10MW WT _s	€-64 mln	€82.71/MWh
Only decommissioning	€-11.7 mln	-

Table 22: LCoE and NPV after 25 years for different systems at Nysted

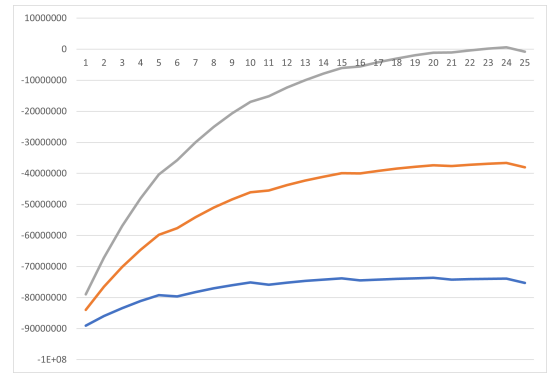
5.3.2 Horns Rev I

The NPV for the first scenario at Horns Rev I is shown in Figure 31a. The NPV for the high price after 25 years is -€8.4 mln. This is slightly better than the AWE systems at Nysted. The wind conditions are similar to Nysted. Therefore, the difference results from the larger number of systems at Horns Rev I, with only a small increase in installation cost. The LCoE for this scenario is €76.89/MWh.

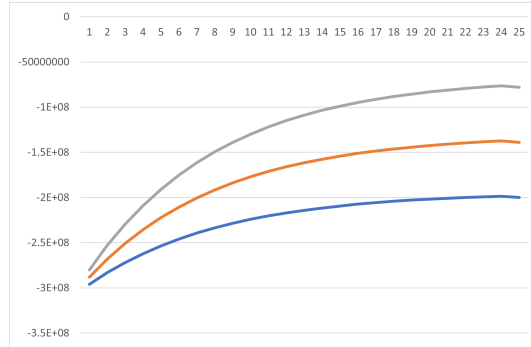
The NPV for the second scenario at Horns Rev I is shown in Figure 31c. After 25 years, the NPV for the high price is -€77.8 mln. Due to the lower OWF efficiency and higher cost at Horns Rev I, this value is lower than the value at Nysted. The LCoE for this scenario is €86.4/MWh.



(a) NPV for AWE on foundation at Horns Rev I



(b) NPV for AWE on the tower at Horns Rev I



(c) NPV for 16 10MW WT_s at Horns Rev I

Figure 31: NPVs for Horns Rev I. Low price: €60/MWh, base price: €80/MWh, high price: €100/MWh

The NPV for the last scenario at Horns Rev I is shown in Figure 31b. The NPV for the high price after 25 years is -€0.8 mln. This is much better than the NPV at Nysted. This difference is again due to the larger number of AWE systems at Horns Rev I at a small cost increase. The improved efficiency due to the lower elevation angle results in larger revenue and a more promising NPV after 25 years. The LCoE for this scenario is €73.46/MWh.

Scenario	NPV after 25 years	LCoE
AWE on foundation	€-9.1 mln	€76.89/MWh
AWE on tower	€-0.8 mln	€73.46/MWh
10MW WTs	€-77.8 mln	€86.37/MWh
Only decommissioning	€-12.6 mln	-

Table 23: LCoE and NPV after 25 years for different systems at Horns Rev I

6 Economic optimization

In Section 5, four scenarios were considered. There are two additional possible scenarios. A possible fifth scenario would be to extend the lifetime of the OWFs until 2MW AWE systems become available. A sixth scenario would be to extend the OWF lifetime with 500kW AWE systems and replace those small systems after 10 years with larger, 2MW AWE systems. This section discovers both possibilities and compares them to the scenarios from Section 5.3.

6.1 Economics 2MW airborne wind energy system

These systems would be more suitable for the size of the foundations and, therefore, could be more profitable. To assess the costs involved in this scenario, a similar approach is taken as in Section 5. The electricity production is calculated with the known data on the wind and assumed characteristics of the 2MW AWE systems. The costs involved are largely based on Section 5.2. In [55], offshore AWE is determined to cost €2.82 mln/MW. This includes the costs of the foundations, substation and array cables. According to [31], the cost of the foundations, substation and array cables contribute to 32% of an OWF. With these values, the cost of a 2MW AWE system is determined to be $I_{AWE} = 2.82 \cdot 10^6 \cdot 2 \cdot (1 - 0.32) = 3.83 \cdot 10^6$. The capacity factors are assumed to be equal to the capacity factors of the smaller systems. This results in the two NPVs for Nysted and Horns Rev I, respectively, in Figure 32.

The LCoE for the installation of 72 2MW AWE systems at Nysted is €54.72/MWh, and for Horns Rev I, the LCoE is €42.48/MWh. This is significantly lower than the LCoE for the 500kW AWE systems. The removal and installation duration and, therefore, the removal and installation costs are unchanged. The higher rated power of the systems comes at a higher cost. However, the larger energy production compensates for this, resulting in a lower LCoE.

These calculations are based on assumptions. Furthermore, the 2MW AWE system is still far away. Therefore, the calculations should be validated carefully in future research. It is recommended to do this research as soon as the 2MW AWE systems are in the prototyping phase.

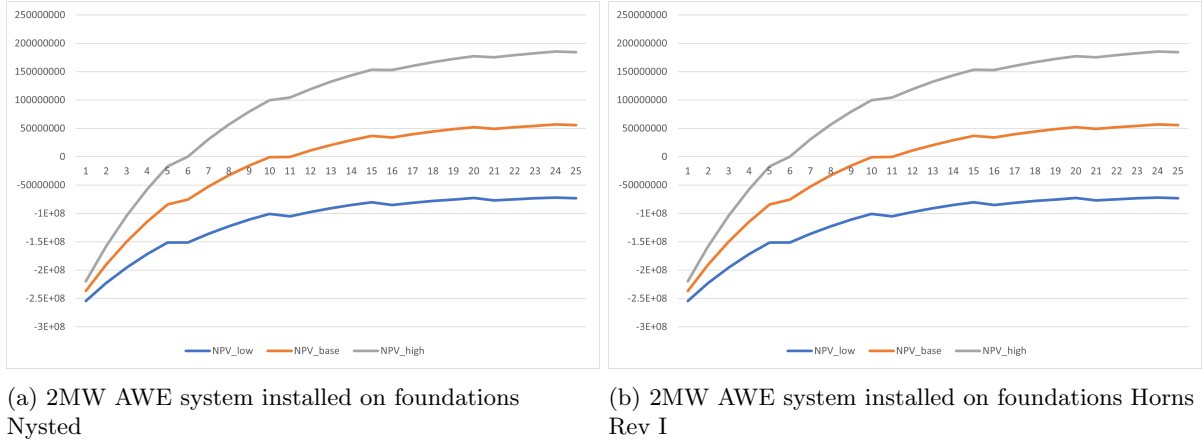


Figure 32: NPVs for 2MW AWE systems

6.2 Economics replacement 500kW AWE with 2MW AWE

A sixth possibility would be to extend the lifetime of the OWFs by initially replacing the WT's with 500kW AWE systems. After 10 years of operation, these 500kW systems could be removed, sold and replaced with 2MW systems. This will increase the electricity production of the OWF and could be profitable. This might be more realistic than the option in Section 6.1 because the 500kW is closer to the market than the 2MW system. In the time the 2MW AWE system is developed, the concept of AWE offshore can be tested with 500kW AWE systems. As soon as the 2MW is ready, the 500kW systems can be replaced with the larger systems. It is assumed that the 500kW AWE systems can be sold after 10 years for 10% of the original costs, saving money in this process. The resulting NPVs for Nysted and Horns Rev I are visible in Figure 33.

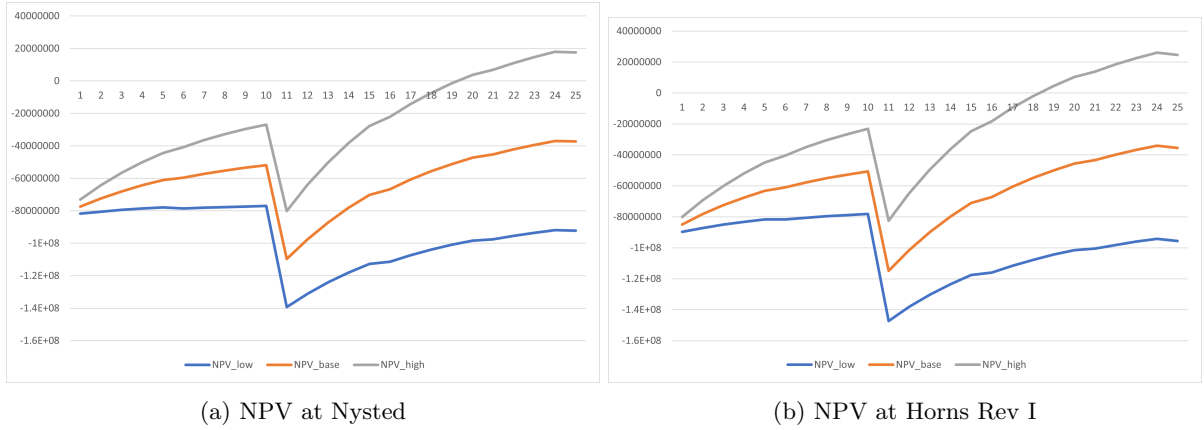


Figure 33: NPVs for initially installing 500kW AWE systems and replacing that with 2MW AWE systems

The LCoE for this scenario, where the 500kW systems are replaced with 2MW AWE systems after 10 years, is €69.13/MWh for Nysted and €67.61/MWh for Horns Rev I. This scenario seems more likely

than the scenario described in Section 6.1. First of all, the 2MW systems are not as close to the market as the 500kW AWE systems. Secondly, with this scenario, the LCoE is lowered by using 2MW systems as soon as they are ready for commercial use. However, it is important to note the timeline of this scenario. It assumes the full development of a 2MW AWE system 10 years after the commercial use of a 500kW AWE system. This might not be realistic, and this should be reconsidered when a more precise timeline of the AWE development is available.

6.3 Reduced discount rate

The discount rate at every calculation is taken conservatively at 7%. As a result, the economics are not promising in terms of NPV. It is possible to calculate the LCoE and NPV with a less conservative discount rate of 5%. This makes quite a difference and results in positive NPVs for the AWE systems, given the calculations are done with the high price. Figure 38 shows the scenarios from Section 5 with a reduced discount rate.

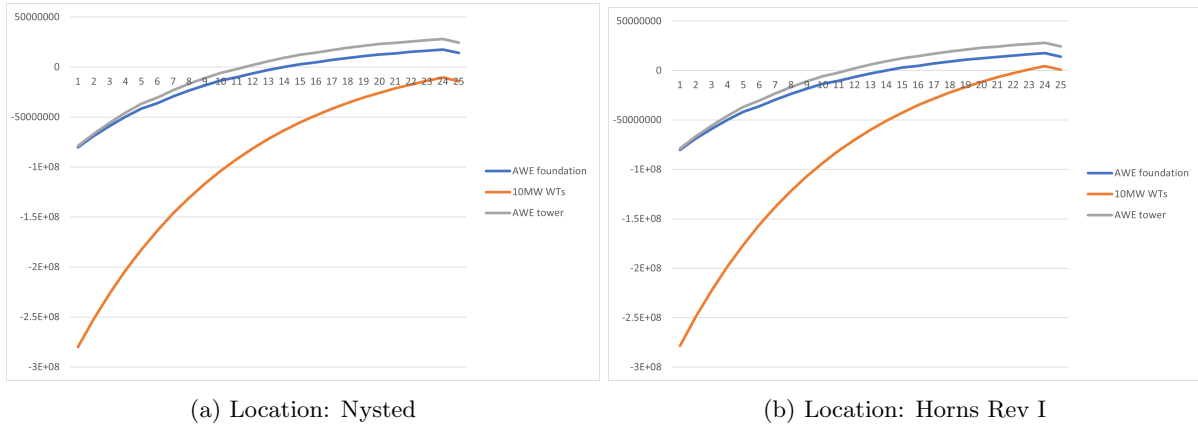


Figure 34: NPVs for both locations with a discount rate of 5% instead of 7%

More details on this can be found in Appendix E, including a table summarizing the results of the reduced discount rate for all the scenarios from Section 5.

6.4 Results

The results from Section 6.1 and Section 6.2 are summarised and compared to the values from Section 5.3 in Table 24. In this table, it is clearly visible that economics involving a 2MW AWE system are more interesting financially. The higher power output, combined with the low additional investment compared to only installing 500kW AWE systems, results in lower LCoEs and more promising NPVs. The table also shows the significant impact of a reduced discount rate of 5%.

	Nysted	Nysted	Horns Rev I	Horns Rev I
Scenario	NPV 25 yrs	LCoE	NPV 25 yrs	LCoE
AWE on foundation	€-16 mln	€85.30/MWh	€-8.4 mln	€76.89/MWh
AWE on tower	€-7.0 mln	€80.74/MWh	€-0.8 mln	€73.46/MWh
10MW WTs	€-64 mln	€82.71/MWh	€-77.8 mln	€86.37/MWh
Only decommissioning	€-11.7 mln	-	€-12.6 mln	-
2MW AWE on foundation	€206 mln	€54.72/MWh	€227 mln	€42.48/MWh
500kW AWE replaced with 2MW AWE	€16.9 mln	€69.13/MWh	€24.6 mln	€67.61/MWh
500kW AWE on foundations 5% discount rate	€2.94 mln	€80.97/MWh	€14.1 mln	€71.59/MWh

Table 24: NPV and LCoE comparison of all systems at Nysted and Horns Rev I

7 Discussion

To limit the scope of this research, assumptions and engineering approaches are used in some cases. This section discusses the limitations of the methods used and gives recommendations for future research. Some of the limitations and the resulting recommendations are based on calculations to check the validity. These calculations are added in Appendix D and E.

7.1 Limitations

There are certain limitations to the methods and calculations used in this research. The most important ones are listed and discussed in this section.

7.1.1 Airbone wind energy system

This report only considers the use of a ground-generating rigid-wing AWE system. This is well reasoned in Section 2.1. However, with additional developments, other AWE systems might be more attractive to use for retrofitting purposes. This could, for example, be the case for the scenario from Section 6.2. For the first 10 years, the possibly cheaper soft kites could be used to be replaced with larger 2MW rigid kites.

For the fatigue calculations in Section 3.3, it is assumed that the tether force fluctuates due to gravity in the shape of a sine wave. A more accurate description of a kite would result in more accurate tether forces and, therefore, more accurate fatigue calculations.

7.1.2 Structural reserves

The calculations on the structural reserves are done with relatively simple models. This limits the accuracy of the calculations. With more data, an extensive model should be made. To account for this, conservative values are chosen in any structural assessment. As a result, the calculated values are on the conservative side.

This research is limited to assumptions on the amount of fatigue damage inflicted on a foundation, expressed as a percentage of allowed fatigue damage to the foundations. As a result, it is difficult to draw a definite conclusion since it is unknown whether or not the foundations have that amount of fatigue damage. With site-specific data on past weather, wind and wave events combined with technical data on the specific OWF, a more realistic model could be made. With this model, the percentages of damage on the structures can be validated. In Appendix D, it is tried to perform such a calculation, with its own many limitations.

If research shows that a tower has too much fatigue damage to be retrofitted with AWE, it could be economically beneficial to reinforce the tower. The AWE system is operating with a higher efficiency when mounted atop the tower. Therefore, it could be worthwhile to invest in reinforcements of the tower to make it structurally possible to mount the AWE systems on top of the tower. Due to the many unknowns on actual tower fatigue damage in this research, calculations reinforcements are only done in an economical sense and can be found in Appendix D.

7.1.3 Economics

The economics are considered extensively, with a revenue and cost analysis. Based on these figures, the LCoE and NPV of each system are calculated. Although the costs and revenue are calculated with as

much precision as possible, there are still a lot of uncertainties. The result is that the cost and income can differ from the calculated values, resulting in different outputs. When a 500kW AWE system is working, it will become clearer if the used values are realistic.

The economic calculations are highly influenced by the discount rate. A lower discount rate results in more promising outcomes. In Section 2, it was shown that a discount rate of 6% is used in the industry. A more conservative discount rate of 7% is used in this research. It is interesting to see the effect of using a lower discount rate. In Appendix E, the calculations for a reduced discount rate of 5% are performed. The reduced discount rate led to significantly more promising results in terms of LCoE and NPV.

For this research, possible subsidies have not been taken into account. Subsidies for projects like this might be possible, but they cannot be counted on. Therefore, the economic calculations are done without any subsidies. However, subsidies could be granted and make a project like this economically more interesting. In Appendix E, the necessary subsidies are calculated.

It is likely that the cost of OWF removal and AWE systems will be going down in the future due to technological advancements and development. This research only considered the costs in the near future. However, as the technology matures, the price will go down. In Appendix E, calculations are performed to indicate the years needed for a more competitive result.

The economics of retrofitting with AWE is compared to repowering with 16 10MW WTs. The results of repowering with WTs are not financially attractive due to the low calculated OWF efficiency. If this OWF efficiency could be increased by 20% to 0.36, it would be as competitive as retrofitting with AWE. This was, however, not within the scope of this research, and it must be emphasized that the economic scenario only serves as a comparison to retrofitting with AWE.

7.1.4 Modifications

This report assumes minimal modifications necessary on the foundations or towers to mount the AWE systems. Furthermore, it assumes that the AWE systems can be manufactured in such a way that they can be bolted onto the foundations or towers with relative ease. It assumes the electrical connections can be made without any difficulties. This might not be realistic and is highly dependent on the OWF that is being retrofitted with AWE.

7.2 Recommendations

This research is an initial feasibility study into the concept of retrofitting OWFs with AWE systems. As a result, many questions arose while doing this research. The most important topics for additional research are listed in this section.

7.2.1 Airborne wind energy

This research is focused on only one AWE system. Research on other AWE systems in a retrofitting context would be interesting as well. Research on AWE is ongoing, and the development of AWE is crucial for the retrofitting of OWFs. Section 6 shows the benefit of a larger AWE system. Therefore, it is very important to ensure the AWE development.

7.2.2 Structural reserves

OWF owners often have the data on weather and waves in the years their OWF was operating. With this data, a structural analysis is possible and accurate damage percentages can be obtained. This is site-specific and should be done when seriously considering retrofitting an OWF with AWE.

7.2.3 Optimization

The electricity production can be elevated by mounting AWE systems atop the foundations. In previous calculations, questions were raised if this was structurally possible. If it is deemed structurally impossible to mount AWE systems atop the tower, modification and reinforcements can be added to the tower and the foundation. In Appendix D, the maximum costs of these modifications are calculated to make it economically viable. Further research can provide insights into whether or not these values are realistic and if it is structurally possible to add these modifications and reinforcements.

7.2.4 Economics

The economic analysis is based on available values. Most of these values are based on assumptions. When there are more insights on the costs of 500kW and 2MW AWE systems, these values should be reconsidered. The same can be said for the cost of decommissioning. With developing technology, the assumed values might not be valid anymore at the time of starting the retrofitting of OWFs with AWE.

8 Conclusion

This report examined various options for retrofitting OWFs with AWE systems. In Section 2, existing literature on the topics of AWE technology and retrofitting OWFs was reviewed. In Section 3, the structural feasibility of mounting the AWE systems on top of the foundations was explored. Section 4 expanded on this by considering the retrofitting of AWE systems on top of the existing tower and the possibility for potentially larger AWE systems. Section 5 discussed the economic aspects of the different systems and compared this to repowering the OWFs with 10MW WTs. Section 6 expanded on this with two additional options of economic optimization. Section 7 discusses the research by showing the limitations and considerations. It also gives recommendations for future research on this topic.

In Section 2, the existing literature was reviewed. There is no existing literature on retrofitting offshore wind foundations with AWE systems. Therefore, a research question was formulated to fill this knowledge gap: Is installing airborne wind energy systems on the monopiles of decommissioned offshore wind farms structurally and economically viable?

In Section 3, it was determined that OWFs are viable for retrofitting with AWE systems. Three case studies were conducted: one reference OWF with conservative input parameters for wind, waves, water depth and foundation diameter, and two real OWFs. The structures were analysed for the fatigue limit state and the ultimate limit state. The ultimate limit state is not exceeded. The maximum allowed fatigue damage of the foundations before retrofitting with AWE was concluded to be over 99%. Therefore, with a remaining fatigue capacity of 1%, the real OWFs and the reference OWF are viable for retrofitting with AWE and will have enough structural reserves to operate for another 25 years.

Section 4 examined possible optimizations of retrofitting with AWE. Mounting the AWE system on top of the tower, therefore only removing the rotors and RNA, was studied. The higher-mounted AWE system would result in a lower elevation angle and, therefore, a more efficient system. This was found to be partially viable. To leave enough structural life for retrofitting with AWE, Nysted could have a maximum of 77% of fatigue damage. For Horns Rev I, this was 43%. This is significantly lower allowed damage than for the AWE on the foundation. However, this might be realistic, and a thorough fatigue study of the locations, with accurate data over the past years, should provide the information needed to determine the viability of retrofitting AWE on top of the tower. It is, therefore, concluded that retrofitting AWE on top of the tower is structurally possible, given low fatigue damage to the structures.

Section 4 also analysed the structural viability of a larger AWE system on the foundation and on top of the tower. A 2MW AWE system was considered due to the similar output to the original installed WTs. It can be concluded that it is structurally possible to retrofit a 2MW AWE system on the foundation. The higher base shear, as a result of the larger tether force, does not exceed the ULS. For the fatigue of the system, this was also not a problem, with allowed fatigue damage of 97.4% to the foundations for Horns Rev I to be viable for retrofitting and an infinite lifetime for Nysted. For the reference OWF, the allowed damage is 96% to be viable for retrofitting with a 2MW AWE system. Retrofitting with a 2MW AWE system atop the tower is impossible. A lifetime of 25 years could not be reached in this scenario, and therefore, it is concluded that this is not an option without reinforcing or replacing the tower. In Section 7, the additional cost and benefit of replacing the tower are discussed.

The economics of retrofitting were analysed in section 5. This section explores the economics of retrofitting the OWFs with AWE systems mounted on the foundation and mounted on the tower. To make a comparison, the economics of a possible competitive system are also analysed: repowering the OWFs with 10MW WTs. To make the analysis, the revenue generated by each system was calculated, taking the

wind velocities and power curves of each location and system into account. The costs of retrofitting were analysed by determining the time and equipment needed to do such operations. The results in terms of LCoE are very promising for each system at €77/MWh for the AWE system on the foundations at Horns Rev I and €85/MWh on the foundations at Nysted. For the AWE systems on top of the tower, the LCoE was even more promising at €73/MWh at Horns Rev I and €81/MWh at Nysted. The 10MW WTs had an LCoE of €87/MWh and €83/MWh, respectively. In the best cases, retrofitting with AWE results in an LCoE that is 2% less than repowering with 10MW WTs at Nysted. At Horns Rev I, retrofitting with AWE results in an LCoE that is 15% less than repowering.

However, the NPVs of the systems were not promising. After their respective lifetimes, none of the systems resulted in positive numbers. With the values used, retrofitting with AWE at Horns Rev I resulted in the lowest LCoE and lowest losses after 25 years, followed by retrofitting with AWE at Nysted. It can be concluded that retrofitting on top of the tower results in an economic benefit due to the higher efficiency. Repowering with 16 10MW WTs is concluded as not viable economically due to the low calculated OWF efficiency. Although the NPVs are not directly promising, it should be noted that the current OWFs must be decommissioned. This is included in the NPVs, but the alternative would be to remove the OWFs and not generate revenue in the following 25 years. It can be concluded that retrofitting with AWE can partially offset the cost of removing OWFs. After 25 years, the costs of decommissioning are higher than the losses generated by retrofitting with AWE. It can therefore be concluded that retrofitting AWE on top of the towers is the most economical way to decommission an OWF.

In Section 4, it was already determined that the foundations are structurally capable of being retrofitted with 2MW AWE systems. In Section 6, this was expanded on economically. Retrofitting with 2MW AWE systems is economically very attractive. The high electricity production, compared with the relatively low cost, made it the most interesting option for retrofitting OWFs with AWE, with an LCoE of €55/MWh at Nysted and €42/MWh at Horns Rev I. However, these systems are not close to being commercially available. Therefore, it is concluded that this is not a realistic possibility.

Therefore, Section 6 also analysed the possibility of initially retrofitting the offshore wind foundations with 500kW AWE system to be replaced with 2MW AWE systems after 10 years. This is more realistic since it gives AWE technology another 10 years for the development of the 2MW systems, while the offshore wind foundations are used with 500kW systems. The result was a positive NPV at both locations for the high price of energy and an LCoE of €69/MWh at Nysted and €68/MWh at Horns Rev I. Upgrading from 500kW to 2MW AWE systems after 10 years significantly reduces LCoE. For Nysted, the reduction is 12%, and for Horns Rev I, the reduction is 19%.

Section 7 discussed the limitations and gave recommendations for future research on this topic related to AWE retrofitting. In the limitations, it showed the importance and effect of the discount rate, learning curve and possible subsidies. Limitations in the structural calculations are also given and expanded on with recommendations.

Retrofitting OWFs with AWE systems is structurally viable for 500kW and 2MW AWE systems. However, when considering AWE systems on top of the towers, a location-specific fatigue analysis is crucial due to lower allowable fatigue damage. Retrofitting AWE systems on top of the tower proves to be the most efficient and economical approach. This approach offers the potential to deploy AWE technology offshore while partially covering the costs of OWF decommissioning, making it a viable option. A more interesting option, financially, is to retrofit OWFs initially with 500kW systems and to replace these systems after 10 years with 2MW AWE systems. The result is a low LCoE and promising NPV after 25 years.

References

- [1] Jacopo Moccia Giorgio Corbetta Iván Pineda. *The European offshore wind industry - key trends and statistics 2013*. URL: https://windeurope.org/wp-content/uploads/files/about-wind/statistics/European_offshore_statistics_2013.pdf.
- [2] URL: <https://map.4coffshore.com/offshorewind/> (visited on 03/16/2023).
- [3] *Global offshore renewable map*. URL: <https://map.4coffshore.com/offshorewind/> (visited on 03/16/2023).
- [4] Ashley M Fowler et al. “Environmental benefits of leaving offshore infrastructure in the ocean”. In: *Frontiers in Ecology and the Environment* 16.10 (July 2018), pp. 571–578. DOI: 10.1002/fee.1827.
- [5] J Sørensen. “Reliability assessment of wind turbines”. In: *Safety, Reliability and Risk Analysis*. CRC Press, Sept. 2013, pp. 27–36. DOI: 10.1201/b15938-5.
- [6] Peng Hou et al. “Offshore wind farm repowering optimization”. In: *Applied Energy* 208 (Dec. 2017), pp. 834–844. DOI: 10.1016/j.apenergy.2017.09.064.
- [7] S. Erlingsson. “Geotechnical Challenges in Iceland”. In: *Proceedings of the XVII European Conference on Soil Mechanics and Geotechnical Engineering* Geotechnical Engineering, foundation of the future (2019), pp. 5196–5220. DOI: 10.32075/17ECSMGE-2019-1109.
- [8] Guy Brindley Lizet Ramírez Daniel Fraile. *Offshore Wind in Europe, Key trends and statistics 2019*. URL: <https://windeurope.org/wp-content/uploads/files/about-wind/statistics/WindEurope-Annual-Offshore-Statistics-2019.pdf>.
- [9] Lizet Ramírez. *Offshore wind energy 2022 statistics*. Tech. rep. 2022. URL: https://proceedings.windeurope.org/biplatform/rails/active_storage/blobs/eyJfcmFpbHMiOnsibWVzc2FnZSI6IkJBaHBBaE1FIiw5beceeeaa9f43d588fdbfd0fb53616525f2e1592c/2022%20WindEurope%20Offshore%20Wind%20Statistics%20Final.pdf.
- [10] P Kirkwood and S Haigh. “Centrifuge testing of monopiles subject to cyclic lateral loading”. In: *ICPMG2014 – Physical Modelling in Geotechnics*. CRC Press, Dec. 2013, pp. 827–831. DOI: 10.1201/b16200-114.
- [11] Cristina Medina, Guillermo M. Álamo, and Román Quevedo-Reina. “Evolution of the Seismic Response of Monopile-Supported Offshore Wind Turbines of Increasing Size from 5 to 15 MW including Dynamic Soil-Structure Interaction”. In: *Journal of Marine Science and Engineering* 9.11 (Nov. 2021), p. 1285. DOI: 10.3390/jmse9111285.
- [12] *Kitemill*. URL: <https://www.kitemill.com/projects> (visited on 03/20/2023).
- [13] IRENA. *Offshore renewables: An action agenda for deployment*. Tech. rep. 2021. URL: https://www.irena.org/-/media/Files/IRENA/Agency/Publication/2021/Jul/IRENA_G20_Offshore_renewables_2021.pdf?rev=9e3ad6549dd44dc9aaaaedae16b747bb.
- [14] European Commission. Directorate General for Research, Innovation., and ECORYS. *Study on challenges in the commercialisation of airborne wind energy systems*. Publications Office, 2018. DOI: 10.2777/87591.
- [15] URL: https://www.startupticker.ch/assets/images/articles/Twingtech_Offshore.jpg (visited on 03/21/2023).
- [16] *13 jaar aan kennis over vliegende windturbines afkomstig van Makani beschikbaar als open source*. URL: <https://www.tudelft.nl/2020/lr/13-jaar-aan-kennis-over-vliegende-windturbines-afkomstig-van-makani-beschikbaar-als-open-source> (visited on 09/11/2023).
- [17] Adrian Gambier. “Retraction Phase Analysis of a Pumping Kite Wind Generator”. In: *Airborne Wind Energy*. Springer Singapore, 2018, pp. 117–135. DOI: 10.1007/978-981-10-1947-0_6.

-
- [18] M. De Lellis et al. “Electric power generation in wind farms with pumping kites: An economical analysis”. In: *Renewable Energy* 86 (Feb. 2016), pp. 163–172. DOI: 10.1016/j.renene.2015.08.002.
- [19] Jochem Weber et al. *Proceedings of the 2021 Airborne Wind Energy Workshop*. Tech. rep. 2021. URL: <https://www.nrel.gov/docs/fy21osti/80017.pdf>.
- [20] Dylan Eijkelfhof and Roland Schmehl. “Six-degrees-of-freedom simulation model for future multi-megawatt airborne wind energy systems”. In: *Renewable Energy* 196 (2022), pp. 137–150. ISSN: 0960-1481. DOI: <https://doi.org/10.1016/j.renene.2022.06.094>. URL: <https://www.sciencedirect.com/science/article/pii/S096014812200934X>.
- [21] Marcelo De Lellis et al. “The Betz limit applied to Airborne Wind Energy”. In: *Renewable Energy* 127 (Nov. 2018), pp. 32–40. DOI: 10.1016/j.renene.2018.04.034.
- [22] Rolf Luchsinger et al. “Pumping Cycle Kite Power with Twings”. In: *Airborne Wind Energy*. Springer Singapore, 2018, pp. 603–621. DOI: 10.1007/978-981-10-1947-0_24. URL: https://doi.org/10.1007/978-981-10-1947-0_24.
- [23] Rolf van der Vlugt, Johannes Peschel, and Roland Schmehl. “Design and Experimental Characterization of a Pumping Kite Power System”. In: *Airborne Wind Energy*. Springer Berlin Heidelberg, 2013, pp. 403–425. DOI: 10.1007/978-3-642-39965-7_23. URL: https://doi.org/10.1007/978-3-642-39965-7_23.
- [24] ‘Early move into new technology’: RWE to test airborne wind energy systems at new Irish site. URL: <https://www.rechargenews.com/wind/early-move-into-new-technology-rwe-to-test-airborne-wind-energy-systems-at-new-irish-site/2-1-1011950> (visited on 08/10/2023).
- [25] *The Kitepower*. URL: <https://i0.wp.com/thekitepower.com/wp-content/uploads/landing-page-bg-min.jpg?fit=2000%2C1325&ssl=1> (visited on 08/10/2023).
- [26] Uwe Fechner and Roland Schmehl. “Model-Based Efficiency Analysis of Wind Power Conversion by a Pumping Kite Power System”. In: *Airborne Wind Energy*. Springer Berlin Heidelberg, 2013, pp. 249–269. DOI: 10.1007/978-3-642-39965-7_14.
- [27] Jochem Weber et al. *Airborne Wind Energy*. Tech. rep. 2021. URL: <https://www.nrel.gov/docs/fy21osti/79992.pdf>.
- [28] Wei He et al. “Innovative alternatives for repowering offshore wind farms”. In: *Journal of Physics: Conference Series* 1618.4 (Sept. 2020), p. 042037. DOI: 10.1088/1742-6596/1618/4/042037.
- [29] A. M. Jadali et al. “Decommissioning vs. repowering of offshore wind farms—a techno-economic assessment”. In: *The International Journal of Advanced Manufacturing Technology* 112.9-10 (Jan. 2021), pp. 2519–2532. DOI: 10.1007/s00170-020-06349-9.
- [30] G. Smith et al. *Assessment of Offshore Wind Farm Decommissioning Requirements*. URL: https://files.ontario.ca/assessment_of_offshore_wind_farm_decommissioning_requirements.pdf.
- [31] BVG associates. *Guide to an offshore wind farm*. the Crown Estate, 2019. URL: <https://www.thecrownestate.co.uk/media/2861/guide-to-offshore-wind-farm-2019.pdf>.
- [32] *Bockstigen Offshore Repowering*. URL: <https://momentum-gruppen.com/case/bockstigen-offshore-repowering/> (visited on 09/28/2023).
- [33] Eva Topham et al. “Recycling offshore wind farms at decommissioning stage”. In: *Energy Policy* 129 (2019), pp. 698–709. ISSN: 0301-4215. DOI: <https://doi.org/10.1016/j.enpol.2019.01.072>. URL: <https://www.sciencedirect.com/science/article/pii/S0301421519300618>.

-
- [34] International Renewable Energy Agency (IRENA). *Innovation outlook: Offshore wind technology*. en. Oct. 2016.
 - [35] *EXPLORATORY RESEARCH AND LCOE OF AIRBORNE OFFSHORE WIND FARM*. URL: <https://topsectorenergie.nl/tki-wind-op-zee/rd-projecten/exploratory-research-and-lcoe-airborne-offshore-wind-farm> (visited on 03/28/2023).
 - [36] Ampyx Power. *The sea-air-farm-project - public summary*. Tech. rep. TKI wind op zee, 2017.
 - [37] Bernard van Hemert. *The sea-air-farm project*. URL: <https://repository.tudelft.nl/islandora/object/uuid:b46e71ef-8e9a-4701-8297-956e122db964/datastream/0BJ/>.
 - [38] Sergio Márquez-Domínguez and John D. Sørensen. “Fatigue Reliability and Calibration of Fatigue Design Factors for Offshore Wind Turbines”. In: *Energies* 5.6 (June 2012), pp. 1816–1834. DOI: 10.3390/en5061816.
 - [39] Maria Luengo and Athanasios Kolios. “Failure Mode Identification and End of Life Scenarios of Offshore Wind Turbines: A Review”. In: *Energies* 8.8 (Aug. 2015), pp. 8339–8354. DOI: 10.3390/en8088339.
 - [40] Lisa Ziegler et al. “Lifetime extension of onshore wind turbines: A review covering Germany, Spain, Denmark, and the UK”. In: *Renewable and Sustainable Energy Reviews* 82 (Feb. 2018), pp. 1261–1271. DOI: 10.1016/j.rser.2017.09.100.
 - [41] Lisa Ziegler. “Assessment of monopiles for lifetime extension of offshore wind turbines”. PhD thesis. July 2018. ISBN: 978-82-326-3208-4.
 - [42] Lisa Ziegler and Michael Muskulus. “Fatigue reassessment for lifetime extension of offshore wind monopile substructures”. In: *Journal of Physics: Conference Series* 753 (Sept. 2016), p. 092010. DOI: 10.1088/1742-6596/753/9/092010.
 - [43] Lisa Ziegler et al. “Brief communication: Structural monitoring for lifetime extension of offshore wind monopiles: can strain measurements at one level tell us everything?” In: *Wind Energy Science* 2.2 (Sept. 2017), pp. 469–476. DOI: 10.5194/wes-2-469-2017.
 - [44] Lisa Ziegler and Michael Muskulus. “Lifetime extension of offshore wind monopiles: Assessment process and relevance of fatigue crack inspection”. In: May 2016.
 - [45] *Pulling Power from the Sky: The Story of Makani*. 2020. URL: https://www.youtube.com/watch?v=qd_hEja6bzE.
 - [46] Paula Echeverri et al. *The Energy Kite - Selected Results From the Design, Development and Testing of Makani’s Airborne Wind Turbines*. Tech. rep. 2020. URL: https://airbornewindeurope.org/wp-content/uploads/2022/04/Makani-2020_TheEnergyKiteReport_Part1-web.pdf.
 - [47] Lorenzo Fagiano et al. “Autonomous Airborne Wind Energy Systems: Accomplishments and Challenges”. In: *Annual Review of Control, Robotics, and Autonomous Systems* 5.1 (2022), pp. 603–631. DOI: 10.1146/annurev-control-042820-124658. URL: <https://doi.org/10.1146/annurev-control-042820-124658>.
 - [48] Lisa Ziegler et al. “Sensitivity of Wave Fatigue Loads on Offshore Wind Turbines under Varying Site Conditions”. In: *Energy Procedia* 80 (2015), pp. 193–200. DOI: 10.1016/j.egypro.2015.11.422.
 - [49] Fabian Vorpahl et al. “Offshore wind turbine environment, loads, simulation, and design”. In: *Wiley Interdisciplinary Reviews: Energy and Environment* 2.5 (Nov. 2012), pp. 548–570. DOI: 10.1002/wene.52.
 - [50] Marc Seidel. “Wave induced fatigue loads”. In: *Stahlbau* 83.8 (Aug. 2014), pp. 535–541. DOI: 10.1002/stab.201410184.

-
- [51] Baran Yeter and Yordan Garbatov. “Structural integrity assessment of fixed support structures for offshore wind turbines: A review”. In: *Ocean Engineering* 244 (Jan. 2022), p. 110271. DOI: 10.1016/j.oceaneng.2021.110271.
 - [52] Jannis Heilmann and Corey Houle. “Economics of Pumping Kite Generators”. In: Oct. 2013, pp. 271–286. ISBN: 978-3-642-39964-0. DOI: 10.1007/978-3-642-39965-7_15.
 - [53] J. Heilmann. *The Technical and Economic Potential of Airborne Wind Energy*. 2012.
 - [54] United Nations. *CDM METHODOLOGY BOOKLET*. 2021. URL: https://cdm.unfccc.int/methodologies/documentation/meth_booklet.pdf.
 - [55] Mike Blanch, Alexi Makris, and Bruce Valpy. *Getting airborne - the need to realise the benefits of airborne wind energy for net zero*. Tech. rep. BVG Associates, 2022.
 - [56] Peter Jamieson. *Innovation in Wind Turbine Design*. Wiley, July 2011. DOI: 10.1002/9781119975441.
 - [57] Junbo Liu et al. “Life cycle cost modelling and economic analysis of wind power: A state of art review”. In: *Energy Conversion and Management* 277 (Feb. 2023), p. 116628. DOI: 10.1016/j.enconman.2022.116628.
 - [58] Morten Kofoed Jensen. *LCOE - Update of recent trends (Offshore)*. Tech. rep. 2022. URL: <https://www.nrel.gov/wind/assets/pdfs/engineering-wkshp2022-1-1-jensen.pdf>.
 - [59] *DNVGL-ST-0437*. 2016.
 - [60] *the windpower*. URL: https://www.thewindpower.net/turbine_en_23_siemens_swt-2.3-82.php (visited on 07/25/2023).
 - [61] *the windpower*. URL: https://www.thewindpower.net/turbine_en_30_vestas_v80-2000.php (visited on 07/25/2023).
 - [62] *DNVGL-RP-C203*. 2014.
 - [63] *DNV-OS-C502*. 2010.
 - [64] *DNV-RP-0416*. 2016.
 - [65] *DNVGL-ST-0126*. 2016.
 - [66] *International standard - ISO19902*. 2007.
 - [67] *The Windpower*. URL: https://www.thewindpower.net/turbine_en_1662_siemens-gamesa_sg-10.0-193-dd.php (visited on 08/01/2023).
 - [68] *Simulated historical climate & weather data for 54.8°N 12.48°E*. URL: <https://www.meteoblue.com/en/weather/historyclimate/climatemodelled/54.803N12.477E> (visited on 08/02/2023).
 - [69] Michiel Kruijff and Richard Ruiterkamp. “A Roadmap Towards Airborne Wind Energy in the Utility Sector”. In: *Airborne Wind Energy*. Springer Singapore, 2018, pp. 643–662. DOI: 10.1007/978-981-10-1947-0_26. URL: https://doi.org/10.1007/978-981-10-1947-0_26.
 - [70] Hidde Vos. *A whole-energy system perspective to floating wind turbines and airborne wind energy in The North Sea region*. 2023. URL: <http://resolver.tudelft.nl/uuid:7bda9c95-1aec-40fb-a585-1e0af8b743bb>.
 - [71] *Neptune - DEME-group*. URL: <https://www.deme-group.com/technologies/neptune#> (visited on 08/05/2023).

A S-N curves

S-N curve	$\log \bar{\sigma}$ For all cycles $m = 3.0$	Thickness exponent k
B1	12.436	0
B2	12.262	0
C	12.115	0.15
C1	11.972	0.15
C2	11.824	0.15
D	11.687	0.20
E	11.533	0.20
F	11.378	0.25
F1	11.222	0.25
F3	11.068	0.25
G	10.921	0.25
W1	10.784	0.25
W2	10.630	0.25
W3	10.493	0.25
T	11.687	0.25 for SCF ≤ 10.0 0.30 for SCF > 10.0

Figure 35: S-N curves for free corroding steel structures

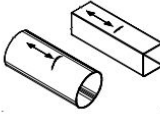
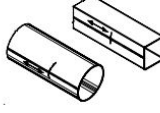
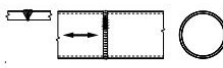
Detail category	Constructional details	Description	Requirement
B1	1. 	1. Non-welded sections	1. — Sharp edges and surface flaws to be improved by grinding
C	2. 	2. Automatic longitudinal seam welds (for all other cases, see Table A-3).	2. — No stop /start positions, and free from defects outside the tolerances of OS-C401 Fabrication and Testing of Offshore Structures.
C1		3. Circumferential butt weld made from both sides dressed flush.	3., 4., 5. and 6. — The applied stress must include the stress concentration factor to allow for any thickness change and for fabrication tolerances, ref. section [3.3.7] . — The requirements to the corresponding detail category in Table A-5 apply.
D		4. Circumferential butt weld made from both sides.	
E		5. Circumferential butt weld made from both sides made at site.	
F		6. Circumferential butt weld made from one side on a backing bar.	

Figure 36: Shapes of steel structures to choose S-N curve

B Formula sheets

In the next pages of this appendix, the formula sheets with useful equations are added. These equations are used throughout this report. The formula sheets are from courses at TU Delft. Specifically: Ocean waves (CIE4325), Bottom founded structures (OE44096) and Motions and loading of structures in waves (MT44021).

LIST OF EQUATIONS

Description of random waves

$$E(f) = \lim_{\Delta f \rightarrow 0} \frac{1}{\Delta f} E\left\{\frac{1}{2}a^2\right\}$$

$$\overline{\eta^2} = \int_0^\infty E(f) df$$

$$H_{1/3} = \frac{1}{N/3} \sum_{j=1}^{N/3} H_j$$

$$A_i = \frac{2}{D} \int_D \eta(t) \cos(2\pi f_i t) dt$$

$$\tan \alpha_i = -\frac{B_i}{A_i}$$

$$\Delta var = \int_{\Delta f} E(f) df$$

$$E(f, \theta) = \lim_{\Delta f \rightarrow 0} \lim_{\Delta \theta \rightarrow 0} \frac{1}{\Delta f \Delta \theta} E\left\{\frac{1}{2}a^2\right\}$$

$$\eta(t) = \sum_{i=1}^N [A_i \cos(2\pi f_i t) + B_i \sin(2\pi f_i t)]$$

$$B_i = \frac{2}{D} \int_D \eta(t) \sin(2\pi f_i t) dt$$

$$a_i = \sqrt{A_i^2 + B_i^2}$$

Short-term wave statistics

$$m_n = \int_0^\infty f^n E(f) df$$

$$p(\eta) = \frac{1}{(2\pi m_0)^{1/2}} \exp\left(-\frac{\eta^2}{2m_0}\right)$$

$$p(H) = \frac{H}{4m_0} \exp\left(-\frac{H^2}{8m_0}\right)$$

$$\overline{f}_\eta = \sqrt{\frac{m_2}{m_0}} \exp\left(-\frac{\eta^2}{2m_0}\right)$$

$$Pr\{\eta_{crest} > \eta\} = \exp\left(-\frac{\eta^2}{2m_0}\right) \quad Pr\{\underline{H} > H\} = \exp\left(-\frac{H^2}{8m_0}\right)$$

$$H_{m_0} \approx 4\sqrt{m_0}$$

Linear wave theory

$$\frac{\partial \mu}{\partial t} + \frac{\partial \mu u_x}{\partial x} + \frac{\partial \mu u_y}{\partial y} + \frac{\partial \mu u_z}{\partial z} = S$$

$$\frac{\partial u_x}{\partial t} = -\frac{1}{\rho} \frac{\partial p}{\partial x}$$

$$\frac{\partial u_y}{\partial t} = -\frac{1}{\rho} \frac{\partial p}{\partial y}$$

$$\frac{\partial u_z}{\partial t} = -\frac{1}{\rho} \frac{\partial p}{\partial z} - g$$

$$\frac{\partial \phi}{\partial t} + \frac{p}{\rho} + gz = 0$$

$$\phi = \hat{\phi} \cos(\omega t - kx)$$

$$u_x = \hat{u}_x \sin(\omega t - kx)$$

$$u_z = \hat{u}_z \cos(\omega t - kx)$$

$$\omega^2 = gk \tanh kd$$

$$c = \omega / k$$

$$\begin{aligned} \frac{\partial(\rho u_x)}{\partial t} + \frac{\partial u_x(\rho u_x)}{\partial x} + \frac{\partial u_y(\rho u_x)}{\partial y} + \frac{\partial u_z(\rho u_x)}{\partial z} \\ = -\frac{\partial p}{\partial x} \end{aligned}$$

$$\frac{\partial u_x}{\partial x} + \frac{\partial u_y}{\partial y} + \frac{\partial u_z}{\partial z} = 0$$

$$\frac{\partial^2 \phi}{\partial x^2} + \frac{\partial^2 \phi}{\partial y^2} + \frac{\partial^2 \phi}{\partial z^2} = 0$$

$$\eta(x, t) = a \sin(\omega t - kx)$$

$$\hat{\phi} = \frac{\omega a \cosh k(d+z)}{k \sinh kd}$$

$$\hat{u}_x = \omega a \frac{\cosh k(d+z)}{\sinh kd}$$

$$\hat{u}_z = \omega a \frac{\sinh k(d+z)}{\sinh kd}$$

$$kd \approx \alpha (\tanh \alpha)^{-1/2}, \quad \alpha = k_0 d = \omega^2 d / g$$

$$c = \frac{g}{\omega} \tanh kd = \sqrt{\frac{g}{k} \tanh kd}$$

Appendix – page 1 (of 2)

Partial Load Factors

	γ_G	γ_Q	γ_E
Permanent and variable actions only	1,3	1,5	0
Extreme conditions when the action effects due to permanent and variable actions are additive	1,1	1,1	1,35
Extreme conditions when the action effects due to permanent and variable actions oppose	0,9	0,8	1,35

Airy wave kinematics for deep and intermediate water

Position along the oblique axis: $s = x \cos \theta + y \sin \theta$

wave elevation: $\zeta = \hat{\zeta} \cos(ks - \omega t)$

velocity potential: $\Phi(s, z; t) = \frac{\hat{\zeta} g}{\omega} \delta_u(z) \sin(ks - \omega t)$

kinematic relations:
$$\begin{cases} u(s, z; t) = \hat{\zeta} \omega \delta_u(z) \cos(ks - \omega t) \\ w(s, z; t) = \hat{\zeta} \omega \delta_w(z) \sin(ks - \omega t) \\ \dot{u}(s, z; t) = \hat{\zeta} \omega^2 \delta_u(z) \sin(ks - \omega t) \\ \dot{w}(s, z; t) = -\hat{\zeta} \omega^2 \delta_w(z) \cos(ks - \omega t) \end{cases}$$

radius of orbital motion: $A = \hat{\zeta} \delta_u(z)$ (half long axis)

$B = \hat{\zeta} \delta_w(z)$ (half short axis)

pressure: $p(s, z; t) = \rho g \hat{\zeta} \delta_p(z) \cos(ks - \omega t) - \rho g z$

Depth-decay functions:

deep water: $\delta_u(z) = \delta_w(z) = \delta_p(z) = e^{kz}$

intermediate water: $\delta_u(z) = \frac{\cosh k(z+d)}{\sinh kd}$, $\delta_w(z) = \frac{\sinh k(z+d)}{\sinh kd}$, $\delta_p(z) = \frac{\cosh k(z+d)}{\cosh kd}$

dispersion relation $\omega^2 = kg \tanh kd$

wave length $\lambda = \frac{2\pi g}{\omega^2} \tanh kd = \frac{gT^2}{2\pi} \tanh kd \approx 1.56 T^2 \tanh kd$

wave celerity: $c = \frac{g}{\omega} \tanh kd = \frac{gT}{2\pi} \tanh kd$

wave height: $H_{\max} \approx 1,86 H_s$

Keulegan-Carpenter Number: $KC = \frac{u_{\text{wave}}^{\max} T}{D} = \pi \frac{H_{\max}}{D}$

Appendix – page 2 (of 2)

Foundation Pile Specifications

	36"	42"	48"	54"	60"	72"
Wall thickness	1,0"	1,75"	2,0"	2,25"	2,5"	2,75"
Ultimate compression*	18,5 MN	22,1 MN	25,1 MN	28,1 MN	31,1 MN	37,3 MN
Ultimate tension*	6,6 MN	7,7 MN	8,9 MN	9,9 MN	11,0 MN	13,2 MN
Ultimate lateral loading*	2,5 MN	3,5 MN	4,5 MN	5,3 MN	6,9 MN	9,4 MN

*) design values for average North Sea conditions

Soil Resistance & Soil Properties

According to the API-code, the shaft-friction capacity Q_{sf} and the end bearing capacity Q_t of an axially loaded pile are respectively found as:

$$Q_{sf} = \frac{A_s}{L} \int_0^L \tau_{sf} dz, \quad Q_t = A_t q$$

Here, τ_{sf} unit skin friction capacity Sand: $\tau_{sf} = \beta \sigma'_{v,0} \leq \tau_{sf,lim}$ Clay: $\tau_{sf} = \alpha s_u$
 q unit end bearing capacity Sand: $q = N_q \sigma'_{v,0} \leq q_{lim}$ Clay: $q = 9s_u$
 $\sigma'_{v,0} = \gamma' z$ effective vertical stress
 A_s pile shaft area
 A_t pile tip area

With: β shaft friction factor 0,5
 γ' effective unit weight of soil [see problem description](#)
 $\tau_{sf,lim}$ shaft friction limit 130 kPa
 α pile-clay friction factor 0,6
 s_u undrained shear strength [see problem description](#)
 N_q end bearing capacity factor 40
 q_{lim} end bearing limit 12 MPa

Soil resistance factors:

$\gamma_{R,ax}$ Axially loaded piles: 1,25
 $\gamma_{R,lat}$ Laterally loaded piles: 1,0

Numerical Integration

Simpson's rule:

$$\int_{z_L}^{z_U} f(z) dz = \frac{z_U - z_L}{6} (f(z_L) + 4f(z_C) + f(z_U)), \quad z_C = \frac{z_U + z_L}{2}$$

- $\cos(a+b) = \cos(a) \cdot \cos(b) - \sin(a) \cdot \sin(b)$
- $\sin(a+b) = \sin(a) \cdot \cos(b) + \cos(a) \cdot \sin(b)$
- $\int x \cos(kx) dx = \frac{kx \sin(kx) + \cos(kx)}{k^2}$
- $\int x \sin(kx) dx = \frac{\sin(kx) - kx \cos(kx)}{k^2}$
- $\int x e^{kx} dx = \frac{1}{k^2} e^{kx} (kx - 1)$
- $\int \cos(\omega t) \sin(\omega t) dt = -\frac{\cos^2(\omega t)}{2\omega}$
- Surface elevation for regular wave with propagation direction μ
 $\zeta(x, y, t) = \zeta_a \cos(kx \cos(\mu) + ky \sin(\mu) - \omega t)$
- Corresponding undisturbed wave potential for regular wave with propagation direction μ in deep water:
 $\Phi_0 = \frac{\zeta_a g}{\omega} e^{kz} \sin(kx \cos(\mu) + ky \sin(\mu) - \omega t)$
- Pressure from Bernoulli equation:
- $p = -\rho \frac{\partial \Phi}{\partial t} - \frac{1}{2} \rho (u^2 + w^2) - \rho g z$
- Forces/Moments from integrated pressures:

$$\vec{F} = - \iint_S (p \cdot \vec{n}) dS$$

$$\vec{M} = - \iint_S p \cdot (\vec{r} \times \vec{n}) dS$$
- Integrated Rayleigh distribution: $P(x > a) = e^{\frac{-a^2}{2m_{ox}}}$
- $e^{-ix} = \cos(x) - i \sin(x)$
- Dispersion relation: $\omega^2 = kg \tanh(kh)$

MT44020 - Part 2 - formula sheet

Trigonometry

$$\cos(\alpha + \beta) = \cos(\alpha) \cos(\beta) - \sin(\alpha) \sin(\beta)$$

Probability density function

$$f_x = \frac{x}{\sigma^2} \exp \left\{ -\frac{x^2}{2\sigma^2} \right\}$$

Drag coefficient

$$C_d = \frac{F}{\frac{1}{2}\rho V^2 A}$$

QTF

$$T(\omega, \omega)^2 = P(\omega, \omega)^2 + Q(\omega, \omega)^2$$

Mean second order wave drift force in irregular waves

$$\overline{F^{(2)}} = 2 \int_0^\infty P(\omega, \omega) S_\zeta(\omega) d\omega$$

Spectral value of the low-frequency second order drift force at frequency μ

$$S_F(\mu) = 8 \int_0^\infty |T(\omega, \omega + \mu)|^2 S_\zeta(\omega) S_\zeta(\omega + \mu) d\omega$$

Spectral value of a response

$$S_R = |H_R(\omega)|^2 S_\zeta$$

Approximation of the variance of surge

$$\sigma_x^2 = \frac{\pi}{2BK} S_F(0)$$

Wall in infinite water depth, per meter length of the wall

$$\overline{F^{(2)}} = \frac{1}{2} \rho g \zeta_a^2$$

Wall with waves under an angle in infinite water depth, per meter length of the wall

$$\overline{F^{(2)}} = \frac{1}{2} \rho g \zeta_a^2 \cos^2 \beta$$

Cylinder with radius R in infinite water depth

$$\overline{F^{(2)}} = \frac{2}{3} \rho g \zeta_a^2 R$$

Incompressible Navier-Stokes equations

$$\nabla \cdot \vec{u} = 0$$

$$\frac{\partial \vec{u}}{\partial t} + \nabla \cdot (\vec{u} \vec{u}^T) - \nu \nabla^2 \vec{u} + \frac{1}{\rho} \nabla p = \vec{F}$$

Bernoulli

$$p = -\rho \frac{\partial \Phi}{\partial t} - \rho g z - \frac{1}{2} \rho (\nabla \Phi)^2$$

Undisturbed wave potential in deep water

$$\Phi(z, x, t) = \frac{\zeta_a g}{\omega} e^{kz} \sin(\omega t - kx)$$

C OWF locations

The map can be found on the next page in full-size.

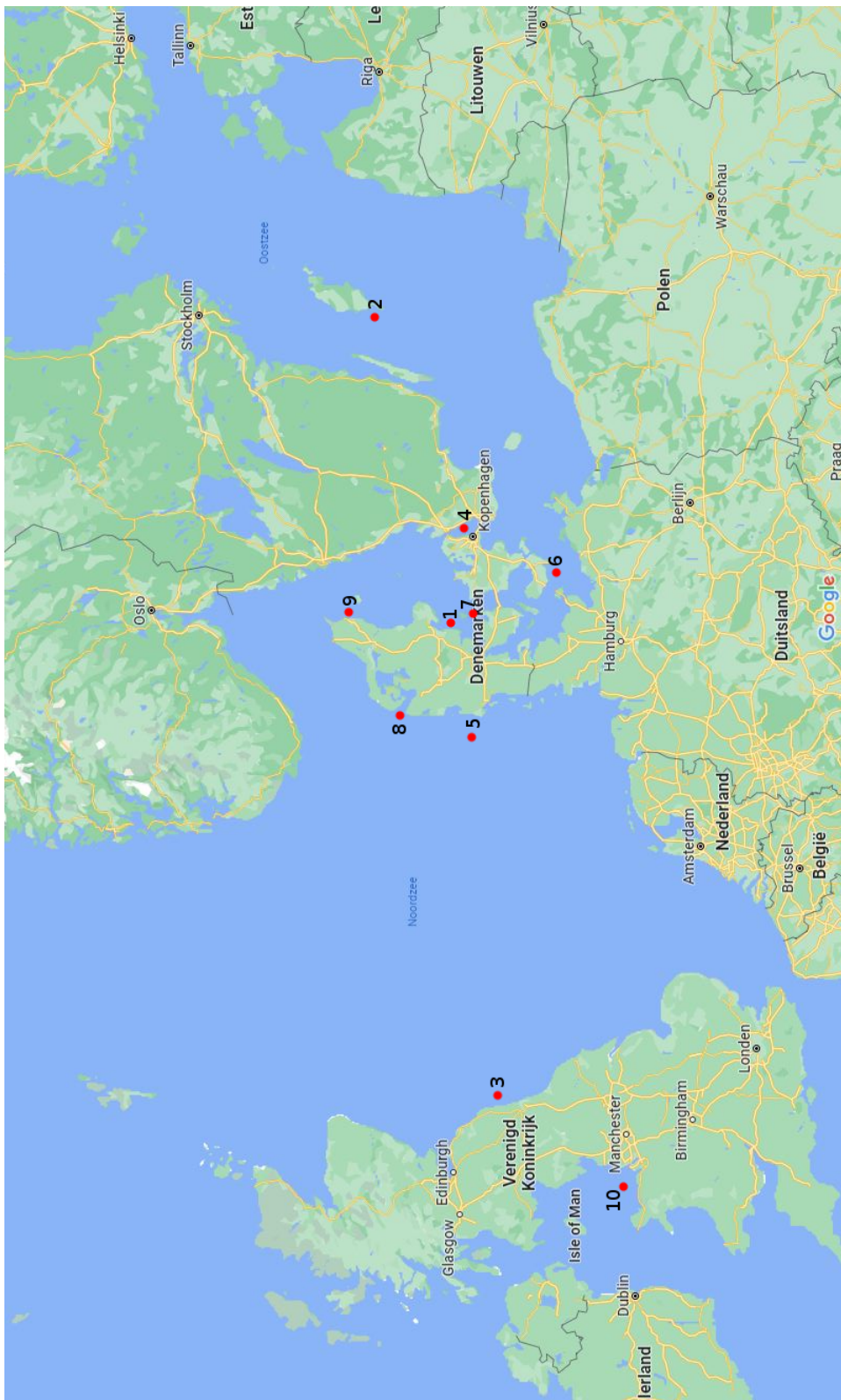


Figure 37: Location of OWFs with more than 20 years of operation[3]

D Structural limitations

D.1 Fatigue damage percentage

This research concluded that AWE systems mounted on the tower are economically very interesting. However, structurally, there is uncertainty about this. With maximum damage of only 43% at Horns Rev I and 77% at Nysted, it was considered structurally viable with enough life left for another 25 years. This results in two questions. Firstly, are 43% and 77% damage realistic values for these OWFs? Secondly, are there options to reinforce the foundations and, more importantly, the towers to ensure a 25-year lifetime for the structures if the damage values are unrealistic? This section will examine both questions and result in an option for future research. The amount of reinforcements to place a 2MW AWE system on top of the tower is examined as well.

To calculate the fatigue damage on the original foundations and towers, a similar approach as in Section 3.3 is used. First, the relevant stresses are determined. The relevant stresses are bending and shear stresses from the waves with the median significant wave height over the past 12 years. This is multiplied by 1.2 for a conservative approach. Furthermore, there are stresses from wind acting on the turbine. The result is a horizontal force at the top of the tower, causing a shear and bending stress. Lastly, there is a moment acting on top of the tower as a result of the velocity changes of the rotor. The stress ranges from the waves are calculated in the same way as in Section 3.1.2. For the stress ranges caused by wind, a different approach had to be taken. The wind is fairly constant in the WTs. Therefore, there is not a large cyclic stress range in the WT. The blades pass the tower three times per revolution, and every full revolution is counted as well. These are known as the 1P and 3P frequencies. This can result in a cyclic loading on top of the tower. For now, it is assumed that the 1P frequency results in a cyclic load of 20% of the maximum horizontal force of 166kN. This load returns every 6.0s. The 3P frequency is assumed to result in a load of 10% of the maximum horizontal force of 166kN and returns every 2.0 seconds. There is a moment acting on top of the tower as well, caused by the change in rotor velocity. It is assumed that the rotor can change 2% of its velocity per passing blade. Furthermore, the cyclic load of changes in wind velocity is taken into account. In Figure 25b, the different wind velocities and the number of hours per year it is that wind velocity are visualised. The mean change in horizontal force per wind velocity, weighted for the hours it is that wind velocity in a year, is calculated at 44.2kN. It is assumed that the wind velocity changes every 6 hours, resulting in another cyclic load. With these values, the total fatigue lifetime of Horns Rev I is 82 years. As a result, after 25 years, Horns Rev I has 30.5% fatigue damage to the structure. The tower at Nysted has 45.5% of fatigue damage as a result of these calculations.

The calculated numbers are promising. However, it is important to note that this is not an accurate way to calculate this. For more accurate results, OWF data is necessary, and a more extensive model should be made to obtain a more realistic result. These calculations only show that it is likely that the OWFs have enough fatigue life left to install AWE systems on top of the tower. It is recommended to do more extensive research on the fatigue life of OWFs, especially the fatigue of the towers and foundations.

D.2 Tower reinforcements

If, after careful analysis, the fatigue damage on the foundations and tower is exceeded, it might be possible to reinforce the structures to increase the expected lifetime and accommodate the AWE systems on top of the tower. For this to make sense financially, the NPV of the AWE systems on the towers, including the cost of the reinforcements, must be higher than the NPV for the AWE systems on the foundations. If it is more expensive to reinforce the towers than the financial benefit it could possibly have, it does not make sense to do this. For Nysted, the total cost of reinforcement can be €9.0 mln, or €125000 per

structure. With this additional investment, the NPV after 25 years is €-16 mln. This is the same as the NPV for AWE on foundations at Nysted. For Horns Rev I, the reinforcement can have a maximum total cost of €8.2 mln, or €102500 per structure, to result in the same NPV as the NPV for AWE on foundations.

The same calculation can be done for the 2MW AWE system on top of the tower. Given the low expected lifetimes of the towers, it is assumed that the towers have to be replaced completely. At Nysted, this results in a higher NPV if this can be done for less than €38 mln in total, or €528000 per structure. For Horns Rev I, this results in a higher NPV if it can be done for less than €40 mln in total or €500000 per structure.

It is recommended to take this into consideration for future research. The higher capacity factor as a result of the lower elevation angle and the resulting additional electricity production is interesting. It can be worth it to reinforce or replace the tower to accommodate an AWE system on top of the tower if this is not possible otherwise.

E Economic limitations

The price of the AWE systems is still very high. This price will go down in the future due to development and the learning curve involved. This section explores the learning curve needed to make retrofitting with 500kW AWE more attractive. This section also dives into the differences a different discount rate can make or how much subsidy is needed to make retrofitting with AWE more attractive.

E.1 Discount rate

A possibility to make retrofitting with AWE systems more interesting is to consider reducing the discount rate. This has to be considered carefully since it can impact the financial picture drastically. With a reduced discount rate from 7% to 5%, the NPV for AWE on foundations at Nysted will be positive after 18 years, assuming the high price of energy of €100/MWh. With the AWE on tower scenario, the NPV is positive after 13 years. Repowering with 16 10MW WT's also is more interesting, with a positive NPV after 22 years. For Horns Rev I, this is after 13 years for AWE on foundations and 11 years for AWE on towers. At Horns Rev I, repowering with 10MW WT's still results in a negative NPV after 25 years. This is the result of the non-ideal wind conditions for 10MW WT's at this site. The NPVs with a 5% discount rate for both locations are visualised in Figure 38. The NPV and LCoE are summarised in Table 25.

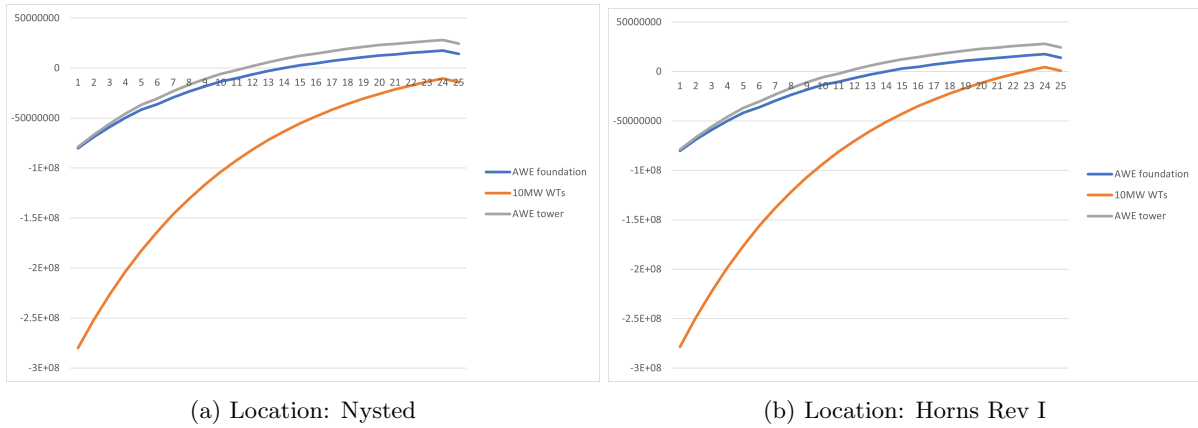


Figure 38: NPVs for both locations with a discount rate of 5% instead of 7%

	Nysted	Nysted	Horns Rev I	Horns Rev I
Scenario	NPV 25 yrs	LCoE	NPV 25 yrs	LCoE
AWE on foundation	€2.94 mln	€80.97/MWh	€14.1 mln	€71.59/MWh
AWE on tower	€13.9 mln	€76.67/MWh	€24.5 mln	€68.45/MWh
10MW WT's	€3.06 mln	€73.70/MWh	€-14.3 mln	€76.96/MWh
Only decommissioning	€-11.7 mln	-	€-12.6 mln	-

Table 25: NPV and LCoE comparison of all systems at Nysted and Horns Rev I with a reduced discount rate to 5%

E.2 Development

This research is based on the calculated assumption that a 500kW AWE system is €950000. It is likely that this price will be lower in the future, with a learning curve. For Nysted, in the scenario that the AWE systems are placed on the foundation, a reduction of 20% of the AWE price is necessary to result in a positive NPV after 25 years. With a conservative learning curve of 3% [55], this reduction will take just over 6 years. At the Nysted location, but with the AWE systems mounted on the tower, a reduction of 7.1% is necessary. With the same learning curve applied, it will take less than 2.5 years for the NPV to result in positive values after 25 years.

For Horns Rev I, a reduction of 8.8% for AWE on the foundations and 1.1% for the AWE on the towers is necessary. A reduction of 8.8% is achieved within 3 years, and a reduction of 1.1% would be achieved within a year. Considering these factors, it might be worthwhile to wait a few years for the technology to develop before employing it on used offshore foundations.

E.3 Subsidy

Another possibility to make retrofitting with AWE more attractive in the near future would be to apply for government subsidies. A subsidy of €13.7 mln for Nysted with AWE on the foundations would result in a positive NPV. For Horns Rev I, with AWE mounted on top of the tower, a subsidy of €836000 is needed. The necessary AWE system price reduction and subsidies to result in a positive NPV are summarised in Table 26.

	Nysted	Nysted	Horns Rev I	Horns Rev I
Scenario	AWE price reduction	Subsidy	AWE price reduction	Subsidy
AWE on foundation	20% (6 years)	€13.7 mln	8.8% (3 years)	€6.69 mln
AWE on tower	7.1% (2.5 years)	€4.86 mln	1.1% (<1 year)	€0.836 mln

Table 26: Necessary AWE price reduction or necessary subsidy